Treating inertia in passive microbead rheology

Tsutomu Indei, Jay D. Schieber, Andrés Córdoba, and Ekaterina Pilyugina

Phys. Rev. E **85**, 021504 — Published 24 February 2012

DOI: 10.1103/PhysRevE.85.021504

On Treating Inertia in Passive Microbead Rheology

Tsutomu Indei, Jay D. Schieber, Andrés Córdoba and Ekaterina Pilyugina

Department of Chemical and Biological Engineering, and

Center for Molecular Study of Condensed Soft Matter

Illinois Institute of Technology

3440 S. Dearborn St., Chicago, Illinois 60616, U.S.A.

Abstract

The dynamic modulus G^* of a viscoelastic medium is often measured by following the trajectory of a small bead subject to Brownian motion in a method called "passive microbead rheology". This equivalence between the positional autocorrelation function of the tracer bead and G^* is assumed via the generalized Stokes-Einstein relation (GSER). However, inertia of both bead and medium are neglected in GSER so that the analysis based on GSER is not valid at high frequency where inertia is important. In this paper, we show how to treat both contributions to inertia properly in one-bead passive microrheological analysis. A Maxwell fluid is studied as the simplest example of a viscoelastic fluid to resolve some apparent paradoxes of eliminating inertia. In the original GSER, the mean-square displacement (MSD) of the tracer bead does not satisfy the correct initial condition. If bead inertia is considered, the proper initial condition is realized thereby indicating an importance of including inertia, but the MSD oscillates as is known, at a time regime smaller than the relaxation time of the fluid. This behavior is rather different from the original result of GSER and what is observed. What is more, the discrepancy from GSER result becomes worse with decreasing bead mass, and there is an anomalous gap between the MSD derived by naïvely taking the zero-mass limit in the equation of motion and the MSD for finite bead mass as indicated by McKinley *et al.* [J. Rheol, **53**, 1487 (2009)]. In this paper, we show what is necessary to take the zero-mass limit of the bead safely and correctly without causing either the inertial oscillation or the anomalous gap, while obtaining the proper initial condition. The presence of a very small purely viscous element can be used to eliminate bead inertia safely once included in GSER. We also show that if the medium contains relaxation times outside the window where the single-mode Maxwell behavior is observed, the oscillation can be attenuated inside the window. This attenuation is realized even in the absence of a purely viscous element. Finally, fluid inertia also affects the bead autocorrelation through the Basset force and the fluid dragged around with the bead. We show that the Basset force plays the same role as the purely viscous element in high frequency regime, and the oscillation of MSD is suppressed if fluid density and bead density are comparable.

I. INTRODUCTION

Microbead rheology is a powerful alternative to measure the linear viscoelastic properties of soft matter [1]. It has become a very popular tool in materials science and biophysics [2–7], and even commercial versions are now available. Unlike bulk rheometers, microbead rheology requires only very small samples. The technique can also be applied to living cells, where no other technique currently exists. The concept is straightforward. In passive microbead rheology, a tracer bead of radius R sufficiently small to be subjected to Brownian motion ($R \lesssim 1\mu$m) is placed in the medium, and the mean-square displacement (MSD)

$$\left\langle \Delta r_{\rm b}(t)^2 \right\rangle_{\rm eq} := \left\langle \left[\boldsymbol{r}_{\rm b}(t) - \boldsymbol{r}_{\rm b}(0) \right]^2 \right\rangle_{\rm eq} \tag{1}$$

of its position $\boldsymbol{r}_{\rm b}$ is followed by using some optical technique. Here t is time, and $\langle \ldots \rangle_{\rm eq}$ is an average taken at equilibrium. Analysis is typically made in the frequency domain via the generalized Stokes-Einstein relation (GSER)

$$\langle \overline{\Delta r_{\rm b}^2}[\omega] \rangle_{\rm eq} = \frac{k_{\rm B}T}{\pi R i\omega G^*(\omega)} \tag{2}$$

where G^* is the dynamic modulus of the medium [8], $k_{\rm B}$ is the Boltzmann constant, T is the temperature, and we indicate the one-sided Fourier transform $\overline{f}[\omega] \equiv \overline{\mathfrak{F}}\{f(t)\} := \int_0^\infty f(t) e^{-i\omega t} dt$ by an overbar and frequency argument ω with square brackets $[\omega]$ (the left side is the abbreviation of $\overline{\mathfrak{F}}\{\left\langle \Delta r_{\rm b}^2(t) \right\rangle_{\rm eq}\}$). Neither bead inertia nor medium inertia are included in GSER. A derivation of eq. (2) is given by Mason in Ref. [9].

Before showing all details, we briefly sketch the derivation of the GSER here, which is comprised of two important relations. One is the Einstein component that relates the MSD and the frequency-dependent friction, or the memory function, $\overline{\zeta}[\omega]$ of the bead in the medium through

$$\langle \overline{\Delta r_{\rm b}^2}[\omega] \rangle_{\rm eq} = \frac{6k_{\rm B}T}{(i\omega)^2 \overline{\zeta}[\omega]}. \tag{3}$$

This is derived from the equation of motion of the bead in the medium when neglecting bead inertia. The other is the Stokes component that connects the memory function and the dynamic modulus of the medium via

$$\overline{\zeta}[\omega] = \frac{6\pi R G^*(\omega)}{i\omega}. \tag{4}$$

This is a generalized version of the Stokes' law so that the frequency-dependent modulus that characterizes viscoelasticity of materials is estimated from the memory function. Medium inertia is not taken into account in this expression. By eliminating $\overline{\zeta}[\omega]$ from both relations, GSER is obtained.

Consider the simplest possible linear viscoelastic fluid, the single-mode Maxwell model $G(t) = g\exp(-t/\lambda)$ with dynamic modulus

$$G^*(\omega) := i\omega\overline{\mathfrak{F}}\{G(t)\} = g\frac{i\omega\lambda}{1+i\omega\lambda}. \tag{5}$$

It is straightforward to insert eq. (5) into eq. (2), and invert the bead displacement back into the time regime to find [10]

$$\left\langle \Delta r_{\rm b}^2(t)\right\rangle_{\rm eq} = \frac{6k_{\rm B}T}{H} + \frac{6k_{\rm B}T}{\zeta}t \tag{6}$$

where $H := 6\pi Rg$ is the spring constant of the elastic component of the Maxwell model and $\zeta := \lambda H$ is the friction coefficient of its viscous component. In the short time regime $t \ll \lambda$, the bead displacement is bounded due to the elastic component of the fluid giving a plateau, while it diffuses away in the long time regime $t \gg \lambda$ due to the viscous component of the fluid. However, *the displacement does not satisfy the proper initial condition*, *i.e.*, $\left\langle \Delta r_{\rm b}^2(t=0)\right\rangle_{\rm eq} = 6k_{\rm B}T/H \neq 0$. This result is clearly anomalous in the sense that it contradicts the definition of $\Delta\boldsymbol{r}_{\rm b}(t)$ at the initial time 0 irrespective of the initial value of $\boldsymbol{r}_{\rm b}(t)$.

If bead inertia is included in GSER, the correct initial condition for the MSD is achieved as shown in Sec. II C. Figure 1 shows the MSD of a bead in the Maxwell fluid calculated from GSER which includes bead inertia. The MSD satisfies the proper initial condition, but it oscillates for $t \lesssim \lambda$ with the frequency $\sim 1/\sqrt{m}$ where m is bead mass [10–13]. The smaller the bead's mass, the higher the frequency of the oscillation so that one recognizes that eq. (6) is never recovered in the zero-mass limit. Such a result is rather different from experimental observation for Maxwell fluids (*e.g.*, wormlike micelle solutions [14–16]); that is, no matter how small the tracer mass is, it has a finite mass that should lead to a highly oscillatory MSD, which is not observed in real systems. These facts give rise to one naïve question: what are the minimal requirements to eliminate inertial effects for Maxwell fluids that are once introduced in GSER? We answer this question here. The effects of both material inertia and bead inertia are considered.

Recently, McKinley *et al.*[12] and Fricks *et al.*[13] studied tracer's individual paths (or positions) and MSD for the memory kernel of the Prony series with an arbitrary number of modes N that corresponds to the generalized Maxwell model. McKinley *et al.*[12] indicated that in the zero-mass

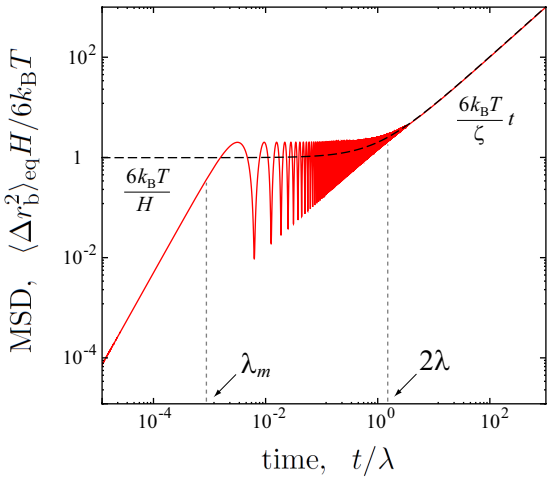

FIG. 1. (color online). Mean-square-displacement of a bead with the mass $m = 10^{-6}\zeta\lambda$ floating in a Maxwell fluid. Dashed line is a result from GSER for the mass-less bead (eq. (6)).

limit of the tracer bead for a fixed finite N, (i) the oscillatory term of the tracer position itself goes to zero in a weak sense, but (ii) this term remains in the MSD giving a finite correction (or anomalous gap) to the MSD, and (iii) this correction vanishes in the limit of $N \to \infty$ for a fixed, finite m. They also detailed the issue of the time window of anomalous diffusive scaling (see also Ref. [17]) which we will not discuss here. In the present paper, we give the essential idea to take the zero-mass limit of the bead safely and correctly without causing either the inertial oscillation nor the anomalous gap as observed in actual viscoelastic fluids and with the proper initial condition. We consider much milder assumptions than do McKinley *et al.*. We show that if the purely viscous component of the solvent is taken into consideration, the oscillation and the anomalous gap of the MSD disappear in the zero-mass limit even for the smallest number of modes $N = 1$, *i.e.*, for the Maxwell fluid. It is not necessary to have multiple modes for the elimination of the oscillation. Methods by McKinley *et al.* and Fricks *et al.* could be extended to add one zero-size relaxation time (*i.e.*, a pure viscosity term), but the critical roles of this term are not considered in their papers. We also discuss the combined effects of bead inertia and fluid inertia, and show that the material inertia tends to suppress the oscillation of the MSD for the Maxwell fluids. Thus, the apparent paradox about the initial condition, anomalous gap and the inertial oscillation for the Maxwell fluid is resolved. It should be emphasized that the elimination of MSD oscillation by the presence of the purely viscous element or fluid inertia is also valid for more realistic systems with a large number of relaxation modes because the broad relaxation spectrum also tends to suppress the oscillation, as already indicated by McKinley *et al.*[12]. Thus, through the study of our ideal

system, we gain a better understanding why these paradoxes are not observed in actual viscoelastic fluids. On the other hand, inertia actually gives sizable effects for real fluids such as worm-like micelle solutions at frequency of order MHz [15]. The GSER that includes tracer inertia and medium inertia can cover this high frequency regime properly in a self-contained way without the help of data from mechanical measurements of the modulus [18]. We treat issues of experimental data analysis in a separate paper.

We discuss the Einstein component of the GSER in the subsequent section. In Sec. II A, we rigorously rederive the Einstein component of GSER that includes the mass of the tracer bead on the basis of the explicitly stationary generalized Langevin equation (GLE). After recalling the equivalence of GLEs with lower limit of the memory integral of either 0 or $-\infty$ in Sec. II B, we revisit the Maxwell fluid in Secs. II C and II D and show that the zero-mass limit of the bead in MSD and the power spectral density (PSD) can be taken safely if a purely viscous component of the fluid is considered. The memory function including a purely viscous component is a novel class of kernels with regularized properties compared to a GLE without this component. The addition of a pure viscous mode suppresses oscillations where the same exponential terms in the kernel would have oscillations, and the zero-mass limit is not singular as it is without the viscous mode. By taking the low-viscosity limit of the purely viscous component *after* the zero-mass limit, the original GSER result, eq. (6), is recovered safely.

Even in the absence of a purely viscous element, the inertial oscillation of the MSD can be attenuated inside the typical experimental time window if there are other modes in the relaxation spectrum outside the frequency window of G^* where the Maxwell behavior is observed. The width of this time window is determined by the relaxation spectrum outside the window. In Sec. II E, we consider the two-mode Maxwell fluid for which one Maxwell mode is inside the experimental frequency window of G^* and the other has frequency outside the window, and seek the conditions where the GSER result for a single-mode Maxwell fluid is recovered. McKinley *et al.* [12] showed that the oscillation tends to decay in the limit of $N \to \infty$. Our results indicate that only a single additional mode is sufficient for the elimination of the oscillation inside the experimental window. The multi-mode systems have been also studied by Fricks *et al.* [13] for the 4-mode Rouse model and the 22-mode Zimm model. In the last part of this section (Sec. II F), we discuss the anomalous gap pointed out by McKinley *et al.* indicating that the inclusion of the purely viscous element can eliminate the gap.

In Sec. III, we discuss the Stokes component of GSER that includes medium inertia. The single-mode Maxwell fluid is again considered as an example to study the effects of fluid inertia

concretely. We show that if fluid density and bead density are comparable, the oscillation of the MSD is suppressed even if there is no purely viscous element in the system. Conclusions are devoted to Sec. IV.

II. EINSTEIN COMPONENT

A. Rederivation of GSER including bead inertia

As in the original paper that introduced the technique [1], we analyze the GSER through the generalized Langevin equation (GLE) for bead position

$$m\frac{d^2\boldsymbol{r}_\mathrm{b}(t)}{dt^2} = -\int_{-\infty}^{t}\zeta(t-t')\frac{d\boldsymbol{r}_\mathrm{b}(t')}{dt'}dt' + \boldsymbol{f}_\mathrm{B}(t), \tag{7}$$

where m is an appropriate mass, $\boldsymbol{f}_\mathrm{B}$ is the Brownian force, and ζ is some as-yet-unspecified memory function. If fluid inertia is not considered, m is purely bead mass, but in the presence of fluid inertia, the mass of fluid dragged around with the bead should be included in m (Sec. III B). We make two important notes. Any spherical Brownian bead in any isotropic medium should be described by the GLE above. An anisotropic medium would have a tensorial $\boldsymbol{\zeta}$. Secondly, most previous attempts to derive the desired expression use $t = 0$ as the lower limit of the integral of eq. (7). Mason derived the expression from such an apparently unstationary GLE but with causality and the equipartition theorem [9]. These conditions are necessary to make a GLE with the lower integral limit 0 stationary at $t \geq 0$. Instead, we employ the explicitly stationary GLE with the lower limit of the integral $-\infty$ to avoid the ill-defined initial condition [19] or unstationarity [20, pp.37-39]. It is shown below that our result is the same as Mason's result when bead mass is not neglected, but we consider our derivation to be more natural. We discuss the choice of the lower limit in Sec. II B.

It can be proven using projection operator technique of Mori [20, pp.97–108] that the Brownian force must have zero mean and satisfy the fluctuation-dissipation theorem (FDT)

$$\langle \boldsymbol{f}_\mathrm{B}(t)\boldsymbol{f}_\mathrm{B}(t')\rangle_\mathrm{eq} = k_\mathrm{B}T\zeta(t-t')\boldsymbol{\delta} \tag{8}$$

where $\boldsymbol{\delta}$ is the identity matrix. In other words, the statistics of the Brownian forces are determined by the memory kernel. For example, if one assumes that the drag force has no memory so that $\zeta(t)$ is a constant times the Dirac delta function $\delta(t)$, eq. (7) reduces to the usual Langevin, or stochastic differential equation.

In the frequency domain, the FDT can be written as

$$\left\langle \boldsymbol{f}_{\mathrm{B}}[\omega]\boldsymbol{f}_{\mathrm{B}}[\omega']\right\rangle_{\mathrm{eq}} = 2\pi k_{\mathrm{B}}T\delta(\omega+\omega')\zeta[\omega]\boldsymbol{\delta}. \tag{9}$$

This relation can be proven by twice taking the inverse two-sided Fourier transform of each side, once for each frequency. Similarly, taking the two-sided Fourier transform of the GLE, eq. (7), we obtain

$$\boldsymbol{r}_{\mathrm{b}}[\omega] = \frac{\boldsymbol{f}_{\mathrm{B}}[\omega]}{-m\omega^2 + i\omega\overline{\zeta}[\omega]}, \tag{10}$$

where $\boldsymbol{r}_{\mathrm{b}}[\omega] = \mathfrak{F}\left\{\boldsymbol{r}(t)\right\} := \int_{-\infty}^{\infty}\boldsymbol{r}(t)e^{-i\omega t}dt$ is the two-sided Fourier transform of bead position. Note that it is the one-sided Fourier transform of the memory kernel ζ that arises here, but the two-sided version in the fluctuation-dissipation theorem, eq. (9). The two-sided Fourier transform for the memory kernel satisfies $\zeta[\omega] = \int_{-\infty}^{\infty}\zeta(t)e^{-i\omega t}dt = 2\Re\left\{\overline{\zeta}[\omega]\right\}$, because ζ is an even function of time, and $\Re\{\ldots\}$ represents taking the real part of the argument.

There exists a relationship between the bead-position autocorrelation in the time and frequency domains similar to that for the Brownian forces, eqs. (8) and (9). Therefore, it is useful to use eq. (10) to write

$$\begin{aligned}\left\langle \boldsymbol{r}_{\mathrm{b}}[\omega]\cdot\boldsymbol{r}_{\mathrm{b}}[\omega']\right\rangle_{\mathrm{eq}} &= \frac{\left\langle \boldsymbol{f}_{\mathrm{B}}[\omega]\cdot\boldsymbol{f}_{\mathrm{B}}[\omega']\right\rangle_{\mathrm{eq}}}{(-m\omega^2+i\omega\overline{\zeta}[\omega])(-m\omega'^2+i\omega'\overline{\zeta}[\omega'])}\\ &= \frac{2d\pi k_{\mathrm{B}}T\delta(\omega+\omega')\zeta[\omega]}{(-m\omega^2+i\omega\overline{\zeta}[\omega])(-m\omega'^2+i\omega'\overline{\zeta}[\omega'])},\end{aligned} \tag{11}$$

where we used the FDT, eq. (9), to obtain the second line, and d is the spatial dimension arising from the inner product in the autocorrelation function. We twice take the inverse Fourier transform of each side to switch back to the time domain

$$\left\langle \boldsymbol{r}_{\mathrm{b}}(t)\cdot\boldsymbol{r}_{\mathrm{b}}(t')\right\rangle_{\mathrm{eq}} = \frac{dk_{\mathrm{B}}T}{2\pi}\int_{-\infty}^{\infty}\frac{\zeta[\omega]e^{i\omega(t-t')}d\omega}{\left|-m\omega^2+i\omega\overline{\zeta}[\omega]\right|^2}. \tag{12}$$

The power spectral-density (PSD) is a two-sided Fourier transform of the autocorrelation function of bead position. By putting $t'=0$ in eq. (12), the PSD is obtained as

$$\begin{aligned}I(\omega) &= \int_{-\infty}^{\infty}\left\langle \boldsymbol{r}_{\mathrm{b}}(t)\cdot\boldsymbol{r}_{\mathrm{b}}(0)\right\rangle_{\mathrm{eq}}e^{-i\omega t}dt\\ &= \frac{2dk_{\mathrm{B}}T\Re\left\{\overline{\zeta}[\omega]\right\}}{\left|-m\omega^2+i\omega\overline{\zeta}[\omega]\right|^2}\\ &= -\Re\left\{\frac{2dk_{\mathrm{B}}T}{i\omega(-m\omega^2+i\omega\overline{\zeta}[\omega])}\right\}.\end{aligned} \tag{13}$$

Equation (10) can also be expressed as

$$\boldsymbol{r}_{\mathrm{b}}[\omega] = \alpha(\omega)\boldsymbol{f}_{\mathrm{B}}[\omega], \tag{14}$$

where $\alpha(\omega) := 1/(-m\omega^2 + i\omega\overline{\zeta}[\omega])$ is the frequency-dependent complex compliance. The PSD, eq. (13), can be rewritten in terms of the complex compliance as

$$I(\omega) = 2dk_{\mathrm{B}}T\frac{|\Im\{\alpha(\omega)\}|}{\omega}. \tag{15}$$

The last equation is the fluctuation-dissipation theorem [21] in d dimensions.

Since bead displacement is a stationary process: $\left\langle r_{\mathrm{b}}^2(t)\right\rangle_{\mathrm{eq}} = \left\langle r_{\mathrm{b}}^2(0)\right\rangle_{\mathrm{eq}}$, the MSD can be expressed in terms of the positional autocorrelation function:

$$\begin{aligned}\left\langle \Delta r_{\mathrm{b}}^2(t)\right\rangle_{\mathrm{eq}} &= 2\left(\left\langle r_{\mathrm{b}}^2(0)\right\rangle_{\mathrm{eq}} - \left\langle \boldsymbol{r}_{\mathrm{b}}(t)\cdot\boldsymbol{r}_{\mathrm{b}}(0)\right\rangle_{\mathrm{eq}}\right)\\ &= \frac{1}{\pi}\int_{-\infty}^{\infty} I(\omega)(1-e^{i\omega t})d\omega.\end{aligned} \tag{16}$$

By taking the two-sided Fourier transform, eq. (16) becomes

$$\left\langle \Delta r_{\mathrm{b}}^2[\omega]\right\rangle_{\mathrm{eq}} = 2\big(I_{\mathrm{total}}\delta(\omega) - I(\omega)\big) = 2\Re\left\{I_{\mathrm{total}}\delta(\omega) + \frac{2dk_{\mathrm{B}}T}{i\omega(-m\omega^2 + i\omega\overline{\zeta}[\omega])}\right\} \tag{17}$$

where $I_{\mathrm{total}} := \int_{-\infty}^{\infty} I(\omega)d\omega = 2\pi\langle r_{\mathrm{b}}^2(0)\rangle_{\mathrm{eq}}$ is the total power of the spectrum. The MSD is an even function due to its stationarity: $\langle \boldsymbol{r}(t)\cdot\boldsymbol{r}(0)\rangle_{\mathrm{eq}} = \langle \boldsymbol{r}(0)\cdot\boldsymbol{r}(-t)\rangle_{\mathrm{eq}}$ and therefore $\langle \Delta r_{\mathrm{b}}^2[\omega]\rangle_{\mathrm{eq}} = 2\Re\{\langle\overline{\Delta r_{\mathrm{b}}^2}[\omega]\rangle_{\mathrm{eq}}\}$, so that eq. (17) is rewritten as

$$\Re\{\langle\overline{\Delta r_{\mathrm{b}}^2}[\omega]\rangle_{\mathrm{eq}}\} = \Re\left\{I_{\mathrm{total}}\delta(\omega) + \frac{2dk_{\mathrm{B}}T}{i\omega(-m\omega^2 + i\omega\overline{\zeta}[\omega])}\right\}. \tag{18}$$

With the help of the Kramers-Kronig relation [21], imaginary parts of $\langle\overline{\Delta r_{\mathrm{b}}^2}[\omega]\rangle_{\mathrm{eq}}$ and $I_{\mathrm{total}}\delta(\omega) + \frac{2dk_{\mathrm{B}}T}{i\omega(-m\omega^2+i\omega\overline{\zeta}[\omega])}$ are obtained uniquely from their real parts, respectively. Since the real parts are equal with each other (eq. (18)), so are the imaginary parts. Therefore, we can conclude

$$\langle\overline{\Delta r_{\mathrm{b}}^2}[\omega]\rangle_{\mathrm{eq}} = I_{\mathrm{total}}\delta(\omega) + \frac{2dk_{\mathrm{B}}T}{i\omega(-m\omega^2 + i\omega\overline{\zeta}[\omega])}. \tag{19}$$

The first term in the right side $I_{\mathrm{total}}\delta(\omega)$ comes from the initial value $\langle r_{\mathrm{b}}^2(0)\rangle_{\mathrm{eq}}$, and is necessary to obtain the correct MSD from the two-sided formulae (16). However, if we use the inverse one-sided Fourier transform (or the Laplace transform for $s := i\omega$) to obtain the time-domain MSD directly from eq. (19), the term $I_{\mathrm{total}}\delta(\omega)$ does not contribute to the result, *i.e.*,

$$\langle \Delta r_{\mathrm{b}}^2(t)\rangle_{\mathrm{eq}} = \overline{\mathfrak{F}}^{-1}\left\{\frac{2dk_{\mathrm{B}}T}{i\omega(-m\omega^2 + i\omega\overline{\zeta}[\omega])}\right\} \tag{20}$$

where $\overline{\mathfrak{F}}^{-1}\{\cdots\}$ represents taking the inverse one-sided Fourier transform of the argument. The last equation is the Einstein component of GSER that takes account of bead inertia. The Einstein component of Mason-Weitz's GSER is derived by just putting $m = 0$ in eq. (20). We usually use eq. (20) to derive the inertial MSD in the time-domain. We assume $d = 3$ in the rest of this paper.

B. Mason's approach

For comparison's sake, we here briefly review Mason's derivation of GSER.

The stationary GLE, eq. (7), can be rewritten as

$$m\frac{d\boldsymbol{v}_{\rm b}(t)}{dt} = -\int_0^t \zeta(t-t')\boldsymbol{v}_{\rm b}(t')dt' + \boldsymbol{f}'_{\rm B}(t), \tag{21}$$

where $\boldsymbol{v}_{\rm b} := d\boldsymbol{r}_{\rm b}/dt$ is bead velocity, and $\boldsymbol{f}'_{\rm B}(t)$ is the effective Brownian force defined by

$$\boldsymbol{f}'_{\rm B}(t) := \boldsymbol{f}_{\rm B}(t) - \int_{-\infty}^0 \zeta(t-t')\boldsymbol{v}_{\rm b}(t')dt'. \tag{22}$$

This Brownian force is not stationary because it depends on the choice of the upper boundary of the time integral (or, equivalently, the lower boundary of the integral in eq. (21)). This property is a "somewhat unnatural artifice" as Kubo *et al.* pointed out in their book [20, pp.37-39]. However, if it satisfies the causality at $t = 0$: $\langle \boldsymbol{v}_{\rm b}(0)\boldsymbol{f}'_{\rm B}(t')\rangle_{\rm eq} = 0$ for $t' > 0$ and the equipartition theorem: $\frac{1}{2}m\langle v_{\rm b}(t)^2\rangle = \frac{3}{2}k_{\rm B}T$ holds for $t \geq 0$, then the autocorrelation function of $\boldsymbol{f}'_{\rm B}$ is stationary and satisfies FDT, and the GLE's, eqs. (21) and (7), describe the same Brownian motion of the bead [20, pp.37-39].

Mason derived the GSER on the basis of eq. (21) with the help of the causality at $t = 0$ and the equipartition theorem while neglecting the bead's mass during the derivation [9]. If bead mass is kept, eq. (20) is obtained by this procedure. This is a consequence of the statistical equivalence between the two GLE's under these two physical conditions.

C. Maxwell fluid

The single-mode Maxwell model is often used to describe the viscoelastic behavior of fluids having a single relaxation time within a certain frequency window, usually at low and moderate frequencies. The dynamic modulus of wormlike micelle solutions [22] and telechelic associating-polymer solutions [23] are well described in terms of the single-mode Maxwell model at lower frequencies. The dynamics of a tracer bead in the single-mode Maxwell fluid has been well studied due to the simple structure of the memory kernel [13, 24]. Here we detail the effects of bead inertia on MSD and PSD for the single-mode Maxwell fluid as an introductory step to investigate the influence of the purely viscous element. Most equations in this section (II C) are already known. Inertial effects of the fluid are not considered here, and we use eq. (4) to relate the memory function to G^* in the rest of this section. Assumptions of eq. (4) and its extension to include fluid inertia is detailed in Sec. III.

The frequency-dependent friction on the bead placed in the Maxwell fluid is obtained by substituting eq. (5) into the Stokes component of GSER, eq. (4). By putting the thus-obtained friction function into eq. (20), we have

$$\langle \overline{\Delta r_{\rm b}^2}[\omega] \rangle_{\rm eq} = \frac{6k_{\rm B}T}{H(i\omega)^2} \frac{1+i\omega\lambda}{\lambda + \lambda_m^2(i\omega) + \lambda\lambda_m^2(i\omega)^2}, \tag{23}$$

where

$$\lambda_m := \sqrt{\frac{m}{H}} \tag{24}$$

is the inertial time scale of bead position. By taking the inverse one-sided Fourier transform of eq. (23), the MSD of the bead is obtained as

$$\left\langle \Delta r_{\rm b}^2(t) \right\rangle_{\rm eq} \simeq \frac{6k_{\rm B}T}{H} \left[1 + \frac{t}{\lambda} - e^{-\frac{t}{2\lambda}} \left(\cos\omega_m t + \frac{3\lambda_m}{2\lambda} \sin\omega_m t \right) \right] \qquad (m \ll \lambda\zeta). \tag{25}$$

It oscillates with frequency ω_m, where

$$\omega_m := \frac{\sqrt{\lambda_m^2 - 4\lambda^2}}{2\lambda\lambda_m} \simeq 1/\lambda_m \quad (m \ll \lambda\zeta). \tag{26}$$

In both eq. (25) and eq. (26), bead mass is assumed to be very small, *i.e.*, $m \ll \lambda\zeta$. This is a rather reasonable assumption. For example, in the microrheological analysis of wormlike micelle solutions that exhibit Maxwellian behavior, typically $m \simeq 10^{-11}\lambda\zeta$. (The plateau modulus and the relaxation time of wormlike micelle solutions are typically $g \simeq 100$Pa and $\lambda \simeq 1$sec, respectively [16], and the bead radius is $R \simeq 1\mu$m. Therefore, $\lambda\zeta = \lambda^2 H = 6\pi R\lambda^2 g \simeq 1$g. On the other hand, bead density is about $\rho_{\rm b} \simeq 1{\rm g/cm}^3$ in many cases, so that the mass of a bead is estimated as $m \simeq 4\pi R^3\rho_{\rm b}/3 \simeq 10^{-11}$g.) In the rest of this paper, we assume the condition $m \ll \lambda\zeta$ and ignore m if it is compared with $\lambda\zeta$, unless otherwise noted.

We now consider the physics behind each time regime of the bead displacement. Equation (25) satisfies the proper initial condition as a result of inclusion of bead inertia. In the short-time regime ($t \ll \lambda_m$), the bead displacement is ballistic, *i.e.*, $\left\langle \Delta r_{\rm b}^2(t) \right\rangle_{\rm eq} \simeq (3k_{\rm B}T/m)t^2$. After the ballistic mode, the MSD oscillates for $\lambda_m \ll t \lesssim 2\lambda$ with frequency ω_m. We assume this oscillatory mode is ascribed to the resonance between the bead motion and the elastic component in the medium. Actually, for purely viscous (Newtonian) fluids in the absence of an elastic trap, oscillations are not generated in the MSD by inclusion of the bead inertia. However, due to the energy dissipation of the bead caused by the viscous component, the oscillation is attenuated after $t \simeq 2\lambda$, and the diffusion motion prevails: $\left\langle \Delta r_{\rm b}^2(t) \right\rangle_{\rm eq} \simeq (6k_{\rm B}T/\zeta)t$. There is no plateau regime in the MSD because the terminal time of the oscillation $\sim 2\lambda$ is longer than the onset of the diffusive

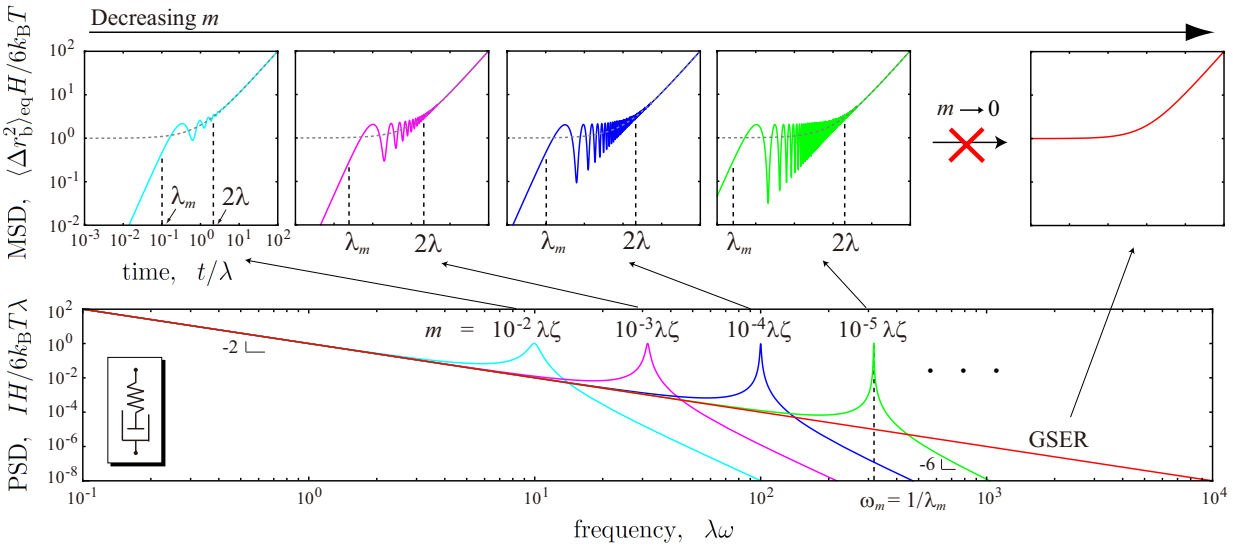

FIG. 2. (color online). The mean-square displacement estimated from eq. (20) and the corresponding power spectral density of a bead embedded in the single-mode Maxwell fluid. A result from GSER is also drawn as a reference.

motion λ (estimated from the coefficient of t in the MSD). In the small-mass limit, the frequency diverges as $1/\sqrt{m}$ while keeping the amplitude of the oscillation finite; therefore the result obtained from GSER, eq. (6), is never recovered (see also Fig. 2). Such a MSD behavior is not observed experimentally for viscoelastic fluids (it can be observed for a viscous fluid, air, when the bead is trapped by an external force [25]).

It is instructive to consider these dynamical properties in terms of the power spectral density. The PSD of the bead is derived from eq. (13) as

$$I(\omega) = \frac{6k_BT}{H\lambda} \frac{\omega_m^4}{\omega^2 \left[(\omega+\omega_m)^2(\omega-\omega_m)^2 + (\omega/\lambda)^2\right]}. \tag{27}$$

Figure 2 shows the PSD and the corresponding MSD for several bead masses. The PSD has a resonance peak at $\omega_m = 1/\lambda_m = \sqrt{H/m}$ with the height $6k_BT\lambda/H$ corresponding to the oscillation of the MSD. Note that the height does not depend on m. At frequencies near the peak, eq. (27) is approximately expressed as

$$I(\omega) \simeq \frac{3k_BT}{2\lambda H} \frac{1}{(\omega-\omega_m)^2 + 1/(2\lambda)^2}. \tag{28}$$

This equation is estimated by putting $\omega = \omega_m$ into eq. (27) other than the term $\omega - \omega_m$ in its denominator. From eq. (28), the half-value width of the peak is known to be $1/\lambda$ independent of m. Thus the area of the peak is not affected by bead mass, and the peak remains no matter how small the bead mass is. On the other hand, a naïve elimination of m annihilates the peak from

the PSD thereby decreasing the total power $I_{\rm total} := \int_{-\infty}^{\infty} I(\omega) d\omega$ by the peak area. This causes an anomalous gap $6k_{\rm B}T/H$ between the MSD derived from eqs. (16) and (13) with $m = 0$ and the MSD from the same equations but for finite m. We discuss the anomalous gap in detail in Sec. II F. Also, eq. (27) is roughly expressed as

$$I(\omega) \simeq \frac{6k_{\rm B}T}{\zeta} \times \begin{cases} \omega^{-2} & (\omega \ll \omega_m) \\ \lambda^2 & (\omega = \omega_m) \\ \omega_m^4 \omega^{-6} & (\omega_m \ll \omega) \end{cases} . \tag{29}$$

At frequency lower than the peak position ($\omega \ll \omega_m$), the PSD is the same as that derived from GSER without bead mass. With decreasing bead mass, the peak at $\omega = \omega_m$ moves towards the higher frequencies with its height and width kept constant, thereby increasing the GSER domain. In the zero-mass limit, the GSER domain extends over the full frequency regime except at the high-frequency extreme where the peak remains, giving rise to the oscillation of MSD with infinite frequency.

D. Effects of solvent viscosity

As stated above, the viscous component of the Maxwell element attenuates the amplitude of the oscillation in MSD at times longer than the relaxation time of the medium due to the energy dissipation of the bead by this viscous component. Therefore, it is reasonable to expect that if a *purely* viscous component exists in the medium, it enhances the attenuation of the oscillation. The purely viscous element often originates from solvent viscosity. We first consider the simplest system of a viscoelastic fluid that includes a purely viscous part: a single Maxwell element and a single purely viscous element connected in parallel (called the three parameter model or the three-element model).

The dynamic modulus of the three-parameter model is

$$G^*(\omega) = g\frac{i\omega\lambda}{1 + i\omega\lambda} + i\omega\eta_0, \tag{30}$$

where η_0 is the viscosity from the purely viscous element. In the following, the friction coefficient of the bead $\zeta_0 = 6\pi R\eta_0$ is used instead of the viscosity to make the equations simple. The memory function of a bead in this fluid can be derived by putting the last equation into eq. (4). Then the MSD in the frequency domain is obtained by substituting the memory function into eq. (20) as

$$\langle \overline{\Delta r_{\rm b}^2}[\omega] \rangle_{\rm eq} = \frac{6k_{\rm B}T}{H(i\omega)^2} \frac{1 + i\omega\lambda}{\lambda + \lambda_0 + (\lambda\lambda_0 + \lambda_m^2)(i\omega) + \lambda\lambda_m^2(i\omega)^2}, \tag{31}$$

where λ_m is the relaxation time of bead position given by eq. (24), and a new time constant

$$\lambda_0 := \frac{\zeta_0}{H} \tag{32}$$

appears that is associated with the purely viscous element of the medium. The power spectral density can be derived from eq. (31) as

$$I(\omega) = \frac{6k_{\rm B}T}{H} \frac{\lambda + \lambda_0 + \lambda_0\lambda^2\omega^2}{\omega^2\left[(\lambda+\lambda_0)^2 + (\lambda_m^4 - 2\lambda_m^2\lambda^2 + \lambda^2\lambda_0^2)\omega^2 + \lambda^2\lambda_m^4\omega^4)\right]}. \tag{33}$$

The inverse one-sided Fourier transform of eq. (31) picks out two poles, the inverse of which describe the characteristic times of the bead floating in the medium. These times are given by

$$\tau_{\rm b,e} := \frac{2\lambda\lambda_m^2}{\lambda\lambda_0 + \lambda_m^2 \pm \sqrt{(\lambda\lambda_0+\lambda_m^2)^2 - 4\lambda\lambda_m^2(\lambda+\lambda_0)}}, \tag{34}$$

where $\tau_{\rm b}$ takes the positive sign and $\tau_{\rm e}$ takes the negative sign. (A subscript b indicates ballistic mode and e stands for elastic plateau.) In the absence of the purely viscous element ($\zeta_0 = 0$), the argument of the square-root of eq. (34), $m(m-4\lambda\zeta)/H^2$, is negative because $m \ll \lambda\zeta$. Therefore, $\tau_{\rm b}$ and $\tau_{\rm e}$ take complex values thereby leading to the oscillation of MSD. However, in the presence of the purely viscous element, the argument of the square root can be positive for a certain range of m meaning that there exists a condition that the MSD does not oscillate. The critical mass m_c for such an oscillation/non-oscillation transition to occur is the mass that makes the square root of eq. (34) zero, and therefore, it is given by

$$m_c := \lambda\zeta\left(\sqrt{1+\lambda_0/\lambda} - 1\right)^2. \tag{35}$$

The MSD does not oscillate if $m < m_c$ while it oscillates if $m > m_c$. (Another root of the equation that makes the square root of eq. (34) zero is $m_c' := \lambda\zeta(\sqrt{1+\lambda_0/\lambda}+1)^2$. This is larger than m_c, and is also always larger than m because $\lambda\zeta \gg m$, so that we can ignore m_c'.)

(i) $m < m_c$: MSD in the time domain is obtained by taking the inverse one-sided Fourier transform of eq. (31). Since $\tau_{\rm b}$ and $\tau_{\rm e}$ are real variables, it is written as

$$\left\langle \Delta r_{\rm b}^2(t) \right\rangle_{\rm eq} = \frac{6k_{\rm B}T}{H}\left(\frac{\lambda}{\lambda+\lambda_0}\right)^2\left[1 + t/\tau_{\rm d} - (1+A_m)e^{-t/\tau_{\rm e}} - A_m e^{-t/\tau_{\rm b}}\right] \tag{36}$$

where $\tau_{\rm d}$ is the longest time-constant with respect to the diffusive mode of the bead:

$$\tau_{\rm d} := \frac{\lambda^2}{\lambda+\lambda_0}, \tag{37}$$

and $A_m := (\frac{\lambda+\lambda_0}{\lambda\lambda_0}\lambda_m)^2$. The bead displacement is classified into four regimes: the ballistic mode ($t \ll \tau_{\rm b}$), a diffusive mode due to the purely viscous element ($\tau_{\rm b} \ll t \ll \tau_{\rm e}$), a plateau by the elastic

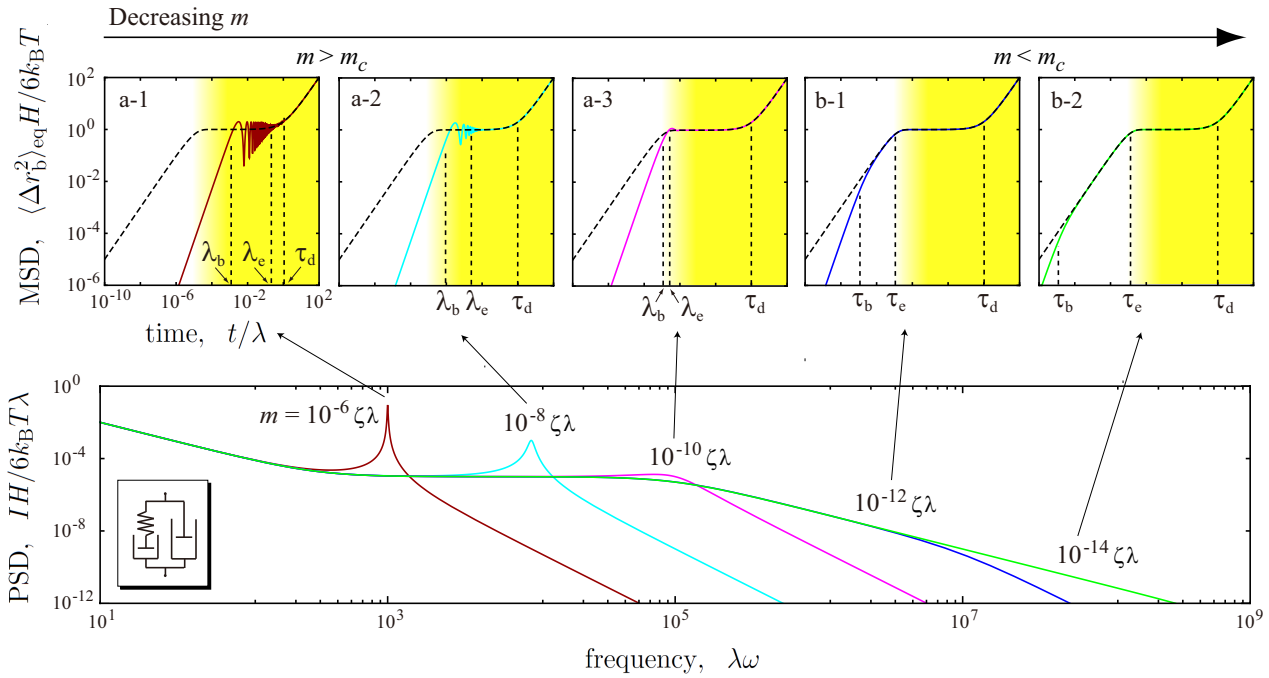

FIG. 3. (color online). The mean-square displacement and the corresponding power spectral density of a bead embedded in the three-parameter model fluid. Dashed curve in each MSD figures are obtained from GSER. The shaded region represents the plateau and succeeding diffusive regime from the GSER. Figures a-1, a-2 and a-3 satisfy the condition $m > m_c$ whereas figures b-1 and b-2 fulfill the opposite condition $m < m_c$. $\zeta_0 = 10^{-5}\zeta$.

element of the Maxwell model ($\tau_e \ll t \ll \tau_d$), and the final diffusive mode due to the two viscous elements of the model ($t \gg \tau_d$). See figures b-1 and b-2 in Fig. 3 for which the bead's mass is so small that the condition $m < m_c$ is attained.

With decreasing bead mass, the ballistic domain is placed in the short-time regime and it disappears in the zero-mass limit (*i.e.*, $\tau_b \simeq m/\zeta_0 \to 0$ with $m \to 0$). Then, noting that $\tau_e \to \frac{\lambda_0\lambda}{\lambda+\lambda_0}$ and $A_m \to 0$, eq. (36) reduces to the MSD derived from GSER for the three-parameter model:

$$\left\langle \Delta r_b^2(t) \right\rangle_{eq} \to \frac{6k_BT}{H}\left(\frac{\lambda}{\lambda+\lambda_0}\right)^2\left(1+\frac{\lambda+\lambda_0}{\lambda^2}t - e^{-\frac{\lambda+\lambda_0}{\lambda\lambda_0}t}\right) \qquad (m \to 0). \tag{38}$$

It is worth mentioning that despite the fact that the last equation is derived with vanishing bead inertia, it satisfies the correct initial condition. This is because the diffusive motion of the bead at shorter time regime ($t \ll \tau_e$) compensates the wrong initial condition. Next, by taking the zero-friction limit of the purely viscous component, then the onset of the plateau goes to 0 (*i.e.*, $\tau_e = \frac{\zeta_0\lambda}{\zeta+\zeta_0} \to 0$ with $\zeta_0 \to 0$), and therefore, eq. (38) approaches the result from the GSER for the Maxwell model (eq. (6)) as shown in Fig. 4. However, unlike eq. (6), the proper initial condition

is satisfied and the MSD jumps at $t = 0$ due to the exponential function of eq. (38), *i.e.*,

$$\left\langle \Delta r_{\rm b}^2(t) \right\rangle_{\rm eq} \to \begin{cases} 0 & (\text{for } t = 0) \\ 6k_{\rm B}T/H + (6k_{\rm B}T/\zeta)t & (\text{for } t > 0) \end{cases} \quad (\zeta_0 \to 0). \tag{39}$$

An important point here is that the zero-mass limit must be taken *before* taking the zero-friction limit so that the result from GSER is achieved correctly for $t > 0$. If the zero-friction limit is taken first, the three-parameter model simply reduces to the single-mode Maxwell model, and does not converge to the original GSER result in the zero-mass limit as explained above.

In real systems where bead mass and the viscosity from the solvent are small but finite, inertial effects appear only in the high-frequency regime.

If we put $m = 0$ in eq. (13) naïvely, the MSD is derived from eqs. (16) and (13) (not from eq. (20)) as $\langle \Delta r_{\rm b}^2(t) \rangle_{\rm eq} = (6k_{\rm B}T/\zeta)t$. This result can be obtained by introducing the harmonic potential to trap the bead around the equilibrium position and then removing it *after* going back to the time domain. This result, $\langle \Delta r_{\rm b}^2(t) \rangle_{\rm eq} = (6k_{\rm B}T/\zeta)t$, satisfies the correct initial condition but there is a constant gap with eq. (39) by $6k_{\rm B}T/H$. This is another pathological result arising from eliminating inertia in a naïve way. This anomalous gap corresponds to the one reported in Ref. [12]. In the presence of an infinitesimal purely viscous element, this paradox is resolved and the gap does not exist anymore, *i.e.*, the MSD becomes expressed as eq. (39). The elimination of the anomalous gap can also be explained in terms of the PSD. In the zero-mass limit, the PSD when there is the small pure viscosity, eq. (33), becomes

$$I(\omega) = \frac{6k_{\rm B}T}{\zeta} \frac{\lambda\omega_0(\omega^2 + \omega_0/\lambda)}{\omega^2(\omega^2 + \omega_0^2)} \tag{40}$$

where $\omega_0 := 1/\lambda_0 = H/\zeta_0$ and the condition $\lambda_0 \ll \lambda$ (or $\zeta_0 \ll \zeta$) is assumed. Equation (40) can be roughly expressed as

$$I(\omega) \simeq \frac{6k_{\rm B}T}{\zeta} \times \begin{cases} \omega^{-2} & (\omega \ll \sqrt{\omega_0/\lambda}) \\ \lambda/\omega_0 & (\sqrt{\omega_0/\lambda} \ll \omega \ll \omega_0) \\ \lambda\omega_0\omega^{-2} & (\omega_0 \ll \omega) \end{cases} . \tag{41}$$

That is, there is a plateau regime in the PSD at $\sqrt{\omega_0/\lambda} \ll \omega \ll \omega_0$ rather than the peak due to the presence of the purely viscous element (see PSD curve for $m = 10^{-14}\zeta\lambda$ in Fig. 3 as a reference). The area of the peak that exists when $m > m_c$ corresponds to the area associated with this plateau regime, and therefore the elimination of the peak by the naive zero-mass limit $m \to 0$ does not create the anomalous gap in the total power $I_{\rm total}$ and thus in the MSD (see Sec. II F for more details).

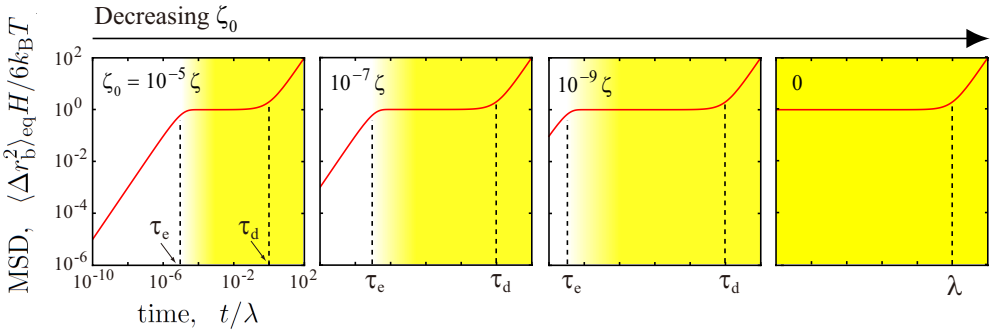

FIG. 4. (color online). The mean-square displacement of a mass-less bead embedded in the three-parameter model fluid. The friction coefficient ζ_0 of the purely viscous element is decreasing from the left to the right figures. In the limit $\zeta_0 \to 0$, the GSER result for the single-mode Maxwell fluid is recovered at $t > 0$ (rightmost figure).

The novelty of this paper is not in the methodology to analyze the oscillation and the time scale (they are found in Refs. [12, 13] for arbitrary number of modes) but in giving the essential idea to take the zero-mass limit safely and correctly without causing either the anomalous gap nor the inertial oscillation with the proper initial condition.

(ii) $m > m_c$: If bead mass is larger than m_c, then τ_b and τ_e are complex variables and therefore MSD is expressed in terms of oscillating functions as

$$\left\langle \Delta r_b^2(t) \right\rangle_{eq} = \frac{6k_BT}{H}\left(\frac{\lambda}{\lambda+\lambda_0}\right)^2\left[1 + t/\tau_d - e^{-\frac{t}{2}\left(\frac{1}{\tau_b}+\frac{1}{\tau_e}\right)}\left(\cos\omega_m t + \frac{\lambda_0}{2\lambda_m^2\omega_m}\sin\omega_m t\right)\right], \quad (42)$$

where the frequency of the oscillation is given as the imaginary part of $1/\tau_{b,e}$, *i.e.*,

$$\omega_m := \frac{\sqrt{4\lambda\lambda_m^2(\lambda+\lambda_0) - (\lambda\lambda_0 + \lambda_m^2)^2}}{2\lambda\lambda_m^2}. \quad (43)$$

The MSD is characterized by the geometric and harmonic mean times rather than τ_b, τ_e themselves, *i.e.*,

$$\sqrt{\tau_b\tau_e} = \lambda_m\sqrt{\frac{\lambda}{\lambda+\lambda_0}} =: \lambda_b, \quad (44)$$

$$\frac{2}{1/\tau_b + 1/\tau_e} = \frac{2\lambda\lambda_m^2}{\lambda\lambda_0 + \lambda_m^2} =: \lambda_e. \quad (45)$$

The bead displacement is classified into four time regimes: the ballistic mode at the shortest time regime $t \ll \lambda_b$, the oscillatory mode at $\lambda_b \ll t \lesssim \lambda_e$ followed by the plateau regime at $\lambda_e \ll t \ll \tau_d$, and the diffusive mode at the longest time regime $t \gg \tau_d$. See figures a-1, a-2 and a-3 in Fig. 3 where the present condition $m > m_c$ is satisfied. The width of the plateau, or a separation of λ_e and τ_d, becomes narrow with decreasing ζ_0, and the plateau disappears in the limit $\zeta_0 \to 0$ because

the onset of the plateau $\lambda_{\rm e}(\to 2\lambda)$ comes later than the terminal $\tau_{\rm d}(\to \lambda)$. Thus the plateau does not exist in MSD for the Maxwell fluid without a purely viscous element.

Relating to the three-element model, it is worth considering here a situation that a tracer bead embedded in a Newtonian fluid is bound by a harmonic potential $\frac{1}{2}H_{\rm e}\delta r_{\rm b}^2$, for example, an externally applied optical trap. Here $\delta \boldsymbol{r}_{\rm b}$ is the bead displacement from its equilibrium position. The MSD of this harmonically bound Brownian particle (HBBP) [26, 27] in the frequency domain is obtained as $\langle\overline{\Delta\delta r_{\rm b}^2}[\omega]\rangle_{\rm eq} = 6k_{\rm B}T/[i\omega(H_{\rm e} - m\omega^2 + i\omega\zeta_0)]$. There is a threshold mass $m_c = \zeta_0^2/(4H_{\rm e})$, above which the MSD oscillates. This oscillation condition can be realized if the medium viscosity is so small as to satisfy $m > m_c$. As a matter of fact, the MSD of a Brownian particle trapped by an optical tweezer in *air* can attain this condition and the MSD oscillates if the air pressure (and therefore viscosity and density) is low [25]. On the other hand, it is impossible for typical liquids to attain such low viscosity. This is one reason why oscillatory behavior of the MSD is not observed for viscoelastic liquids.

E. Effects of relaxation spectrum outside experimental window

So far, we have focused on the simplest fluidal system that has only a single viscoelastic relaxation time λ. In general, however, viscoelastic fluids exhibit a more complex relaxation spectrum with multiple modes. It is natural to expect that short relaxation times in the spectrum contribute to the damping of the oscillation of MSD as the purely viscous component does for the Maxwell fluid. We show here that the broad spectrum that contains a short relaxation time *outside* the frequency window of G^* in which a single-mode Maxwellian behavior is observed can attenuate the oscillation of MSD *inside* the corresponding time window. Thus, the GSER's result is approximately recovered inside the window even in the absence of the purely viscous element.

As the simplest example, we consider the two-mode Maxwell model whose dynamic modulus is described by

$$G^*(\omega) = g_1\frac{i\omega\lambda_1}{1+i\omega\lambda_1} + g_2\frac{i\omega\lambda_2}{1+i\omega\lambda_2}. \tag{46}$$

We assume that the first mode with relaxation time λ_1 and modulus g_1 is greatly separated in time from the second mode with relaxation time λ_2 and modulus g_2, *i.e.*, $\lambda_1 \gg \lambda_2$, so that each Maxwell mode is discernible. By taking the limit $\lambda_2 \to 0$ while keeping the viscosity $\eta_2 = g_2\lambda_2$ constant, the second mode reduces to the purely viscous element. Thus the present two-mode model is a simple extension of the three-parameter model discussed in Sec. II D, but this model helps us obtain an

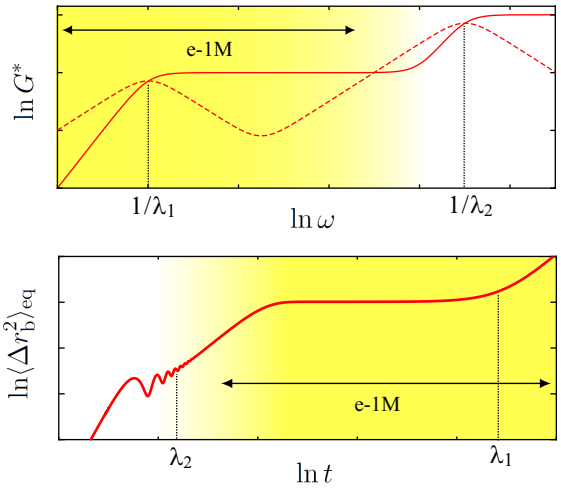

FIG. 5. (color online). The dynamic modulus of the discernible two-mode Maxwell fluid (top) and an example of the mean-square displacement of the bead embedded in it (bottom). The shaded domain describes the extended single-mode Maxwell (e-1M) window $\omega \ll 1/\lambda_2$ or $t \gg \lambda_2$. The second Maxwell mode can attenuate the oscillation of the MSD inside the e-1M window (see text).

insight into more general multi-mode systems.

In the following, we focus on a window defined by the frequency domain $\omega \ll 1/\lambda_2$, or by the time domain $t \gg \lambda_2$. We call it the e-1M (extended single-mode Maxwell) window because this window includes not only the first Maxwell mode but a transient regime between two modes (see Fig. 5). The second Maxwell mode strongly influences the MSD inside the e-1M window. An employment of such an extended window is reasonable since the experimental window of G^* for Maxwell fluids such as wormlike micelle solutions observed by conventional mechanical rheometer often includes higher frequency modes.

By putting eq. (46) into eq. (20), MSD of a bead embedded in the two-mode Maxwell fluid is obtained in the frequency domain as

$$\langle \overline{\Delta r_{\rm b}^2}[\omega] \rangle_{\rm eq} = \frac{6k_{\rm B}T}{(i\omega)^2} \frac{1 + (\lambda_1 + \lambda_2)i\omega + \lambda_1\lambda_2(i\omega)^2}{\zeta_1 + \zeta_2 + (\lambda_1\zeta_2 + \lambda_2\zeta_1 + m)i\omega + m(\lambda_1 + \lambda_2)(i\omega)^2 + m\lambda_1\lambda_2(i\omega)^3}, \quad (47)$$

where $\zeta_j := \lambda_j H_j$ $(j = 1, 2)$ is the friction coefficient of the viscous component of each Maxwell mode with $H_j := 6\pi R g_j$ being the spring constant of each elastic component. We reasonably assume a condition $m \ll \lambda_1\zeta_1$ as before, as well as $\lambda_1 \gg \lambda_2$.

It is useful to separate eq. (47) into two parts, for inside and outside the e-1M window to good approximation as

$$\langle \overline{\Delta r_{\rm b}^2}[\omega] \rangle_{\rm eq} \simeq \langle \overline{\Delta r_{\rm b}^2}[\omega] \rangle_{\rm eq}^{(1)} + \langle \overline{\Delta r_{\rm b}^2}[\omega] \rangle_{\rm eq}^{(2)}. \quad (48)$$

This separation makes the denominator of eq. (47) quadratic and therefore the method employed in Sec. II D can be applied. The first term

$$\langle\overline{\Delta r_{\rm b}^2}[\omega]\rangle_{\rm eq}^{(1)} := \frac{6k_{\rm B}T}{(i\omega)^2}\frac{1+i\omega\lambda_1}{\zeta_1+\zeta_2+(\lambda_1\zeta_2+\lambda_2\zeta_1+m)i\omega+m\lambda_1(i\omega)^2} \tag{49}$$

$$= \frac{6k_{\rm B}T}{m(i\omega)^2}\frac{i\omega+1/\lambda_1}{\left(i\omega+1/\tau_{\rm b}^{(1)}\right)\left(i\omega+1/\tau_{\rm e}^{(1)}\right)} \tag{50}$$

describes the behavior inside the e-1M window $\omega \ll 1/\lambda_2$. Equation (49) is derived by approximating $\lambda_1+\lambda_2 \simeq \lambda_1$ and by neglecting the highest order term of ω in both the denominator and numerator of eq. (47). Singular points of eq. (50) give (the inverse of) the bead's characteristic times in the fluid at $t \gg \lambda_2$. They are

$$\tau_{\rm b,e}^{(1)} := \frac{2m\lambda_1}{\lambda_1\zeta_2+\lambda_2\zeta_1+m \pm \sqrt{(\lambda_1\zeta_2+\lambda_2\zeta_1+m)^2-4m\lambda_1(\zeta_1+\zeta_2)}} \tag{51}$$

where $\tau_{\rm b}^{(1)}$ ($\tau_{\rm e}^{(1)}$) takes the positive (negative) sign. On the other hand, the second term in the right side of eq. (48) describes the behavior outside the e-1M window $\omega \gg 1/\lambda_2$ and is given by

$$\langle\overline{\Delta r_{\rm b}^2}[\omega]\rangle_{\rm eq}^{(2)} := \frac{6k_{\rm B}T}{i\omega}\frac{\lambda_1\lambda_2}{\lambda_1\zeta_2+\lambda_2\zeta_1+m+m\lambda_1(i\omega)+m\lambda_1\lambda_2(i\omega)^2}$$

$$= \frac{6k_{\rm B}T}{mi\omega}\frac{1}{\left(i\omega+1/\tau_{\rm b}^{(2)}\right)\left(i\omega+1/\tau_{\rm e}^{(2)}\right)}, \tag{52}$$

where

$$\tau_{\rm b,e}^{(2)} := \frac{2m\lambda_1\lambda_2}{m\lambda_1 \pm \sqrt{(m\lambda_1)^2-4m\lambda_1\lambda_2(\lambda_1\zeta_2+\lambda_2\zeta_1+m)}} \tag{53}$$

are bead characteristic times at $t \ll \lambda_2$ for which $\tau_{\rm b}^{(2)}$ ($\tau_{\rm e}^{(2)}$) takes the positive (negative) sign. This term is obtained by neglecting the first and the second terms in the numerator and the first term in the denominator of eq. (47).

Typical behaviors of the MSD are shown in Fig. 6 for several different bead masses. Mathematical descriptions of the MSD and details of relevant time constants in Fig. 6 are given in App. A. There are two critical masses $m_c^{(1)}$ and $m_c^{(2)}$ defined by eq. (A4) and eq. (A11), respectively. If $m > m_c^{(1)}$, the MSD oscillates in the e-1M window. With decreasing bead mass, the oscillatory regime becomes narrow, and it disappears if $m = m_c^{(1)}$. The oscillation is pushed outside the e-1M window if $m < m_c^{(1)}$. Thus the second Maxwell element outside the first Maxwell window drives the oscillation to the outside of the window in which GSER's result is recovered at a large part ($t \gg \tau_{\rm e}^{(1)}$). The condition for the oscillation to occur in each side of the window is summarized in Tab. I. Note that if $m_c^{(2)}$ is smaller than $m_c^{(1)}$ and a condition $m_c^{(2)} < m < m_c^{(1)}$ is satisfied,

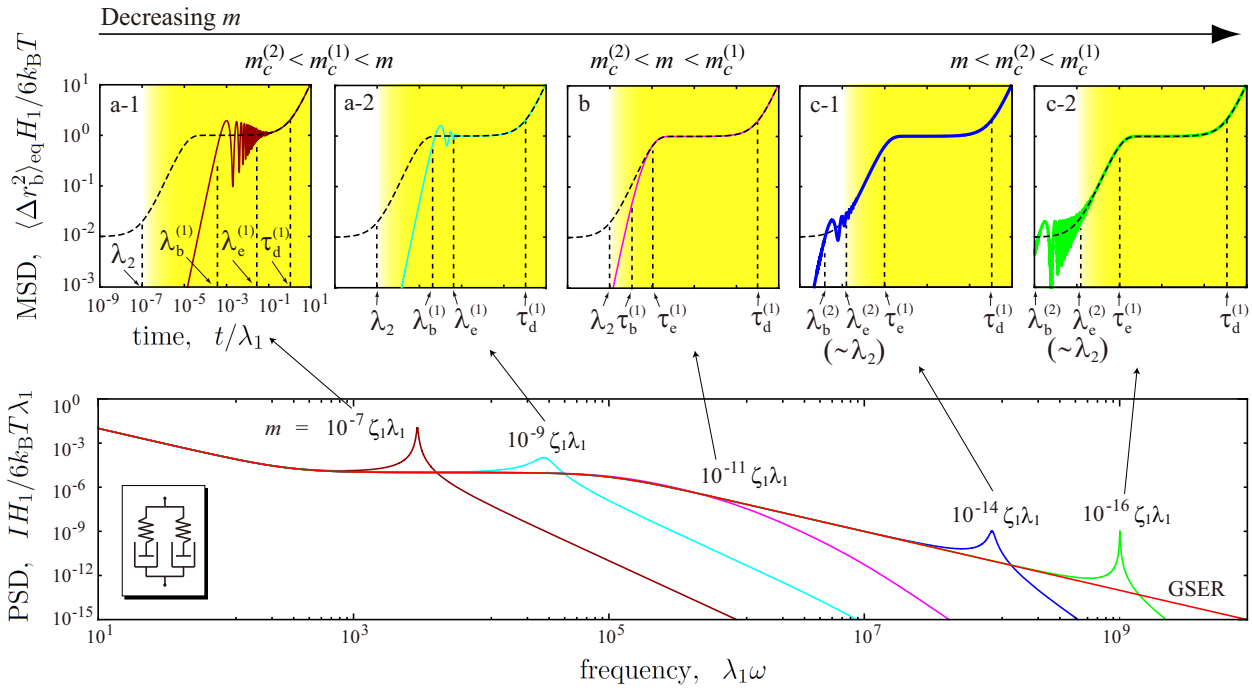

FIG. 6. (color online). The mean-square displacement and the corresponding power spectral density of a bead embedded in the two-mode Maxwell fluid. Dashed curve in each MSD figure is drawn from GSER without bead mass. The shaded domain describes the e-1M window $t \gg \lambda_2$. In figures a-1 and a-2, bead mass satisfies the condition $m_c^{(2)} < m_c^{(1)} < m$. In figure b, a condition $m_c^{(2)} < m < m_c^{(1)}$ is satisfied. Figures c-1 and c-2 fulfill the inequality $m < m_c^{(2)} < m_c^{(1)}$. See also the left table in Tab. I. $\lambda_2 = 10^{-7}\lambda_1$ and $\zeta_2 = 10^{-5}\zeta_1$.

then the MSD does not oscillate over all time regimes as shown in figure b of Fig. 6. On the other hand, if $m_c^{(2)}$ is larger than $m_c^{(1)}$ and $m_c^{(1)} < m < m_c^{(2)}$ is fulfilled, the oscillation occurs across the boundary of the observable window (not shown here).

The oscillation inside the e-1M window ($t \gg \lambda_2$) shifts towards shorter times outside the window with decreasing bead mass. The shifted oscillation never disappears outside the e-1M window. But if there is a third Maxwell mode with the relaxation time λ_3 smaller than λ_2, it shifts further towards the shorter time regime as bead mass decreases. In general, the broader the relaxation spectrum, the smaller the time regime where the oscillation takes place in MSD. This is another reason why the oscillations of the MSD are typically not observed and GSER works properly inside experimental windows in real systems.

		OUTSIDE	INSIDE
a.	$m_c^{(2)} < m_c^{(1)} < m$	$\surd$	oscillate
b.	$m_c^{(2)} < m < m_c^{(1)}$	$\surd$	$\surd$
c.	$m < m_c^{(2)} < m_c^{(1)}$	oscillate	$\surd$

		OUTSIDE	INSIDE
d.	$m_c^{(1)} < m_c^{(2)} < m$	$\surd$	oscillate
e.	$m_c^{(1)} < m < m_c^{(2)}$	oscillate	oscillate
f.	$m < m_c^{(1)} < m_c^{(2)}$	oscillate	$\surd$

TABLE I. The condition for the oscillation not to occur in MSD for the inside ($t \gg \lambda_2$) and the outside ($t \ll \lambda_2$) of the e-1M window for $m_c^{(2)} < m_c^{(1)}$ (left) and $m_c^{(1)} < m_c^{(2)}$ (right). $\surd$ means that the oscillation does not occur.

F. Anomalous gap in the zero-mass limit

McKinley *et al.* [12] studied the singular nature of the zero-mass limit for the generalized Maxwell model of an arbitrary number of modes with uniform and random weights. They started from the GLE with the lower integral limit 0, and calculated the bead position in the Laplace space. Then they derived the bead position (or path) in the time domain by taking the inverse Laplace transform with keeping m finite (a), or by naïvely putting $m = 0$ (weak zero-mass limit) before the transformation (b), and showed that both results do not agree even in the long time regime where the inertial oscillation decays. The result is shown in Fig.3 of Ref. [12] for the 16-mode Rouse model. McKinley *et al.* showed that this anomalous gap disappears in the limit of infinite number of modes $N \to \infty$.

Due to the equivalence of GLEs stated in Sec. II B, the same goes for the MSD derived from the GLE (7) with the lower integral limit $-\infty$. That is, the MSD derived from eqs. (16) and (13) with keeping m finite (a) is larger than the MSD obtained from these equations by naïvely putting $m = 0$ before the integration (b) in the time regime where the oscillation decays. See Fig. 7 where the results for the two-mode Maxwell model are shown. For the generalized Maxwell model ($\overline{\zeta}[\omega] = \sum_j \frac{\zeta_j}{1+i\omega\lambda_j}$), the anomalous gap $\delta_{\rm MSD}$ is estimated to be

$$\delta_{\rm MSD} = \lim_{t\to 0}\langle \Delta r_{\rm b}^2(t)\rangle_{\rm eq} = \frac{6k_{\rm B}T}{\sum_j H_j} \tag{54}$$

where the inverse one-sided Fourier transform of $\lim_{\omega\to\infty}\langle\overline{\Delta r_{\rm b}^2}[\omega]\rangle_{\rm eq} = \frac{6k_{\rm B}T}{i\omega\sum_j H_j}$ (see eq. (20) with $m = 0$) was taken in the second equality. We can explain this gap in terms of the inertial peak of the PSD as follows. (The following discussion is based on the analytical results for $N = 1$ and numerical results for $N = 2, 3, 4$ for wide range of parameter-value sets of $\{\lambda_j, \zeta_j\}$, but it could be generalized to any N in a straightforward manner.) In the case of (a) (*i.e.*, $m > 0$), there is an inertial peak in the PSD as previously shown for the Maxwell fluids (Sec. II C). On the other hand, the procedure (b) (*i.e.*, naïvely put $m = 0$) eliminates the peak in the PSD. Therefore, the

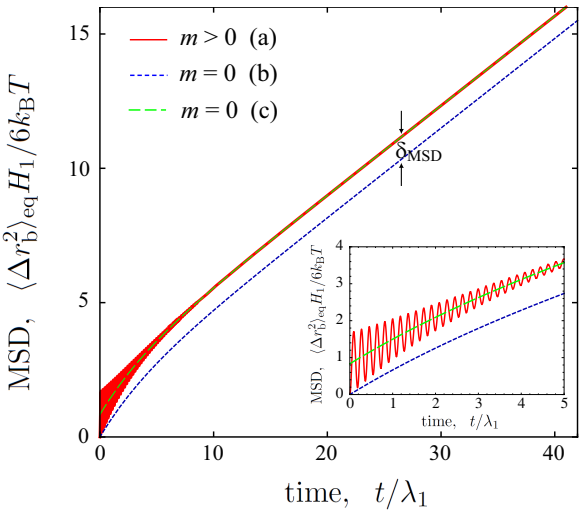

FIG. 7. (color online). The mean-square displacement of the bead in the two-mode Maxwell fluid derived from eqs. (16) and (13) for the finite bead mass $m = 10^{-3}\lambda_1\zeta_1$ (a), from the same equations but taking the zero-mass limit naïvely in the frequency domain (b), from Mason-Weitz's GSER ($t > 0$) that takes the zero-mass limit naïvely in the frequency (or Laplace/one-sided Fourier) domain (c). Although (b) and (c) should give the same result because they are seemingly the same procedure, there is a gap $6k_{\rm B}T/(H_1 + H_2)$. By introducing the infinitesimal pure viscosity and then taking the zero-mass limit in the frequency domain, the gap can be eliminated and (b) becomes (c). In the limit of the infinite number of modes $N \to \infty$, (c) approaches (b) (not opposite) as $6k_{\rm B}T/\sum_{j=1}^{N} H_j \to 0$. This figure can be compared with Fig. 3 of Ref. [12]. $\zeta_2 = 2\zeta_1,\ \lambda_2 = 10\lambda_1$.

total area under the PSD curve $I_{\rm total} = \int_{-\infty}^{\infty} I(\omega)d\omega = 2\pi\langle r_{\rm b}^2(0)\rangle_{\rm eq}$ for (b) is smaller than that for (a) by the peak area $\delta I_{\rm total}$:

$$I_{\rm total}^{(b)} = I_{\rm total}^{(a)} - \delta I_{\rm total}. \tag{55}$$

Or, equivalently, $\langle r^2(0)\rangle_{\rm eq}$ for (b) is smaller than that for (a) by $\delta I_{\rm total}/(2\pi)$:

$$\langle r^2(0)\rangle_{\rm eq}^{(b)} = \langle r^2(0)\rangle_{\rm eq}^{(a)} - \delta I_{\rm total}/(2\pi). \tag{56}$$

Recalling that the MSD is written as $\langle \Delta r_{\rm b}^2(t)\rangle_{\rm eq} = 2\langle r_{\rm b}^2(0)\rangle_{\rm eq} - 2\langle \boldsymbol{r}_{\rm b}(t)\cdot\boldsymbol{r}_{\rm b}(0)\rangle_{\rm eq}$, the MSD for (b) (*i.e.*, $m = 0$) is smaller than that for (a) (*i.e.*, $m > 0$) by the gap $\delta I_{\rm total}/\pi$ that is estimated to be

$$\begin{aligned}\delta I_{\rm total}/\pi &= (I_{\rm total}^{(a)} - I_{\rm total}^{(b)})/\pi \\ &= \frac{1}{\pi}\int_{-\infty}^{\infty} \left(I(\omega)|_{m>0} - I(\omega)|_{m=0}\right) d\omega \\ &= 6k_{\rm B}T\left(\frac{1}{\sum_j H_j} - \frac{m}{(\sum_j \zeta_j)^2}\right).\end{aligned} \tag{57}$$

Note that $I_{\rm total}$ is a divergent quantity due to the singularity of $I(\omega)$ at $\omega = 0$ by the diffusive nature of the bead in the long-time limit, but the difference of inertial $I_{\rm total}|_{m>0}$ and inertia-less $I_{\rm total}|_{m=0}$ is finite. We treat mathematical details in a separate paper. Equation (57) becomes equal to MSD gap given by eq. (54) when $m \ll (\sum_j \zeta_j)^2 / \sum_j H_j$. Even if we take the zero-mass limit in (a), the inertial peak in the PSD just shifts towards the high frequency and never disappears as previously shown for the Maxwell fluids, and therefore the MSD for $m > 0$ (a) never approaches that for $m = 0$ (b) no matter how small m is. If there is a pure viscosity in the dynamic modulus, the peak in the PSD decays in the zero-mass limit. But the area from the pure viscosity compensates the peak area of the PSD, so that the gap of the MSD does not appear. Thus the correct result can be obtained by adding the infinitesimal viscosity before taking the zero-mass limit (c).

The Einstein part of Mason-Weitz's GSER derives the correct inertia-less MSD at $t > 0$ as (c) by the *one-sided* Fourier transform in spite of the fact that the zero-mass limit is taken naïvely as (b). This is because the term $I_{\rm total}\delta(\omega)$ in eq. (19) disappears by taking the inverse one-sided Fourier transform and therefore $\delta I_{\rm total}$ does not affect the MSD in the time-domain.

III. STOKES COMPONENT

A. Correspondence principle

Expressions (13) and (20) relate the measurable quantity on the left with the response of the fluid to the bead $\zeta(t)$. More typically, we seek the material property of the medium instead of its response to a particular probe. Hence, we seek a relationship between the memory kernel $\zeta(t)$ and the appropriate material property. It is here where we necessarily make assumptions that restrict the applicability of the relations. First, we assume that the bead experiences a continuous medium, which implies that the bead radius R is larger than the fluid microstructure. Second, we assume that the fluid is incompressible. A network in a solvent is expected to show compression from bead motion, and would require a different approach [28]. Thirdly, we assume that the viscous solvent and solute are coupled through viscous drag and move as one at length scales large compared with the fluid microstructure [29]. Finally, we assume that, since the bead experiences only Brownian forces and no external driving forces, the fluid remains near equilibrium so is completely characterized by its linear viscoelastic (LVE) properties. LVE theory states that all rheological information is contained in the relaxation modulus $G(t)$, or equivalently the dynamic modulus $G^*(\omega)$ [8]. Since we are near equilibrium we assume that terms of the equation of motion that are nonlinear in

velocity can be neglected. Our final assumption restricts us to passive microbead rheology, or very small perturbations in active microbead rheology.

The memory kernel $\zeta(t)$ in the GLE is a macroscopic quantity that can be determined by solving the flow field around a bead sphere. In the paper of Schnurr, *et al.* [29], an explanation is given for the generalization of Stokes Law to a viscoelastic medium. Basically, the idea is that the viscosity in the solution of the problem for a sphere moving in the medium can be replaced by $G^*/(i\omega)$. This (correct) idea is explained in the paper through the concept of a compressible network. We show it in a more general and mathematically explicit way.

The correspondence principle mentioned in that paper [29] between low-Reynolds number, purely viscous flow, and linear viscoelasticity is made much more explicit in a recent paper [30]. However, that paper [30] is restricted to steady-state flow only, so does not cover the problem at hand. The correspondence was seen as early as 1970 by Zwanzig and Bixon [31], when they applied the idea to exactly the problem of a bead in a viscoelastic medium. In their paper they restricted the relaxation spectrum to a single mode. The original connection between Stokes flow and LVE appears to have been made with solid mechanics by Lee [32]. We now consider the general time-dependent case.

Conservation of momentum in an incompressible viscoelastic fluid yields the equation of motion

$$\rho \frac{\partial \boldsymbol{v}(\boldsymbol{r},t)}{\partial t} = -\nabla \cdot \boldsymbol{\tau}(\boldsymbol{r},t) - \nabla p(\boldsymbol{r},t) \tag{58}$$

where ρ is the fluid density, $\boldsymbol{v}(\boldsymbol{r},t)$ is the fluid velocity field at a location $\boldsymbol{r}$, ∇ is the vector differential, $\boldsymbol{\tau}$ is the stress tensor, $p(\boldsymbol{r},t)$ is pressure, and terms nonlinear in velocity are neglected. Equation (58) requires a constitutive equation relating stress to the flow field. For an incompressible Newtonian fluid, this expression is

$$\boldsymbol{\tau}(\boldsymbol{r},t) = -\eta \left[\nabla \boldsymbol{v}(\boldsymbol{r},t) + (\nabla \boldsymbol{v}(\boldsymbol{r},t))^\dagger \right]. \tag{59}$$

Any general viscoelastic medium near equilibrium can be described by the LVE constitutive equation

$$\boldsymbol{\tau}(\boldsymbol{r},t) = -\int_{-\infty}^{t} G(t-t') \Big[\nabla \boldsymbol{v}(\boldsymbol{r},t') + (\nabla \boldsymbol{v}(\boldsymbol{r},t'))^\dagger \Big] dt', \tag{60}$$

where $G(t)$ is the relaxation modulus. The key to the correspondence is that eqs. (58-60) are linear in both velocity and stress. Hence, we can take the two-sided Fourier transform of both sides of the last three equations. Then the equation of motion for the Newtonian and LVE fluids have the same form in the frequency domain

$$\rho i\omega \boldsymbol{v}[\omega] = \eta^*(\omega) \nabla^2 \boldsymbol{v}[\omega] - \nabla p[\omega], \tag{61}$$

where $\eta^*(\omega) := \eta$ for the Newtonian fluid and $\eta^*(\omega) := G^*(\omega)/(i\omega)$ for the LVE fluid. The argument $\boldsymbol{r}$ of both $\boldsymbol{v}$ and p is omitted for simplicity. For our problem, both fluids are expected to have the same (sticky) boundary conditions $\boldsymbol{v}(|\boldsymbol{r}| = R) = d\boldsymbol{r}_\mathrm{b}/dt$, so the spatial dependence of the solution to each problem is the same—only the time (or frequency) dependence is different. Therefore, to obtain the LVE prediction from the creeping flow solution, we just have to transform the creeping flow solution to the frequency domain, and make the substitution: $\eta \to \eta^*(\omega) = G^*(\omega)/(i\omega)$. This last observation has great practical importance: any Newtonian creeping-flow solution can be used to find the solution for the LVE problem. Since a great number of analytic solutions and efficient numerical techniques exist for creeping flow, these may be taken over directly into LVE.

B. Medium inertia

Landau and Lifshitz [33] give a detailed solution of eq. (61) for the Newtonian fluid for the force $\boldsymbol{F}$ on a sphere surface. Zwanzig and Bixon [31] claim that Stokes derived the essential elements for the solution in 1851, and that the following was first found by Boussinesq

$$\boldsymbol{F}[\omega] = \left\{ 6\pi R\eta + 6\pi R^2\sqrt{\rho i\omega\eta} + \frac{2}{3}\pi R^3 \rho i\omega \right\} i\omega \boldsymbol{r}_\mathrm{b}[\omega]. \tag{62}$$

The first term on the right side is the well-known Stokes-law drag term for steady displacement, the second is the Basset force [34], and the third is the inertia of the fluid that is dragged along with the bead [35]. We chose the sign for the square root so that the power spectral density has positive values for all frequencies. Note that sign for $i\omega$ in the Fourier transform is different from that of Ref. [33] thereby causing a different coefficient in the Basset force from that of Ref. [33].

If we take the Fourier transform of eq. (7) and compare to eq. (62), we obtain

$$\overline{\zeta}[\omega] = 6\pi R\eta + 6\pi R^2\sqrt{\rho i\omega\eta} \tag{63}$$

for the Newtonian fluid. Note that we have added fluid inertia as an effective mass to the bead, which is appropriate. Hence, m in eq. (7) should be replaced with

$$m_\mathrm{eff} := m + M/2 \tag{64}$$

where $M := \frac{4}{3}\pi R^3\rho$ is the medium mass per bead volume. To obtain the memory kernel for the LVE fluid, we make our substitution $\eta \to G^*(\omega)/(i\omega)$

$$\overline{\zeta}[\omega] = \frac{6\pi R G^*(\omega)}{i\omega} + 6\pi R^2\sqrt{\rho G^*(\omega)} \tag{65}$$

for the LVE fluid. Note that the expression assumed in earlier work does not contain the second term. This term can be neglected if $\omega \ll \omega_M$ where ω_M is determined by

$$\sqrt{\frac{|G^*(\omega_M)|}{\rho R^2}} = \omega_M. \tag{66}$$

When a rigid body in a Newtonian fluid moves and disturbs its surroundings, the stress penetrates through the fluid. Propagation of the stress is characterized as the diffusion of a vortex. In the case of an oscillatory disturbance with frequency ω, the vortex expands away from the body to a distance of the penetration depth (or oscillatory boundary layer) $\delta = \sqrt{\eta/(\rho\omega)}$ [33, 36]. For a viscoelastic material, the penetration depth is approximately $\delta = \sqrt{|G^*|/(\rho\omega^2)}$ [30]. If R is much smaller than δ, effects of fluid inertia and stress propagation are negligible. This leads to the condition $\omega \ll \omega_M$. In other words, inertial effects of the material become strong at frequencies higher than ω_M. For example, for aqueous solutions of wormlike micelles, G^* is typically $10^2 \sim 10^3$Pa in the high-frequency domain and $\rho \sim 1\text{g/cm}^3$ [15]. Since particle size is order one micron, the critical frequency for fluid inertia is about $\omega_M \simeq 10^5 \sim 10^6$rad/sec in this system which is attainable in a recent technique [37].

Equation (65) is quadratic in $\sqrt{G^*}$, so solution is straightforward

$$G^*(\omega) = \frac{i\omega\overline{\zeta}[\omega]}{6\pi R} + \frac{R^2\omega^2}{2}\left(\sqrt{\rho^2 + \frac{2\rho\overline{\zeta}[\omega]}{3\pi R^3 i\omega}} - \rho\right). \tag{67}$$

The second term comes from the Basset force, which goes to 0 in the limit $\rho \to 0$. The sign for the square root can be determined from the condition that G' and G'' must be positive. Therefore, only the plus sign is possible.

C. Maxwell fluid

We again consider the single-mode Maxwell fluid but now taking account of fluid inertia together with bead inertia.

There are two types of contribution from the fluid inertia: one is the Basset force and the other is the inertia of the fluid dragged around with the bead. The Basset force appears in the memory function that is given by putting eq. (5) into eq. (65) as

$$\overline{\zeta}[\omega] = \zeta\left(\frac{1}{1+i\omega\lambda} + \frac{1}{\lambda\omega_M}\sqrt{\frac{i\omega\lambda}{1+i\omega\lambda}}\right) \tag{68}$$

where

$$\omega_M = \frac{\sqrt{2}}{3}\sqrt{\frac{H}{M}} \tag{69}$$

is the frequency defined by eq. (66) above which the Basset force affects bead displacement. In the following we consider the frequency regime $\omega \gg 1/\lambda$ because we are interested in inertial effects which appear only at high frequency (note that $\omega_M \gg 1/\lambda$). In this condition, $\sqrt{i\omega\lambda(1+i\omega\lambda)} \simeq \pm i\omega$ and therefore eq. (68) is approximately

$$\overline{\zeta}[\omega] \simeq \frac{\zeta}{1+i\omega\lambda}\left(1+\frac{i\omega}{\omega_M}\right) \qquad (\omega\lambda \gg 1). \tag{70}$$

The second term in the parentheses, that proportional to $\sqrt{M}$, comes from the Basset force. The sign for this term must be plus so that the PSD is positive for all ω. On the other hand, the inertia of the dragged fluid contributes to the PSD through the effective mass $m_{\rm eff} = m + M/2$:

$$I(\omega) = -\Re\left\{\frac{6k_{\rm B}T}{i\omega(-m_{\rm eff}\omega^2 + i\omega\overline{\zeta}[\omega])}\right\} \tag{71}$$

where m in eq. (13) was replaced with $m_{\rm eff}$. The fluid density and the bead density should be comparable so that the bead undergoes Brownian motion in the fluid. Thus the ratio $M/m = \rho/\rho_{\rm b}$ takes a value of order one. Below, we take a look at these influences of fluid inertia on the PSD one at a time.

1. *Effects of the Basset force*

Firstly, we examine the effects of the Basset force alone. By putting eq. (70) into the last equation but with $m_{\rm eff} = 0$, we obtain

$$I(\omega) \simeq \frac{6k_{\rm B}T}{\zeta}\frac{\lambda\omega_M(\omega^2+\omega_M/\lambda)}{\omega^2(\omega^2+\omega_M^2)} \qquad (\omega \gg 1/\lambda). \tag{72}$$

This expression is the same as that for the single-mode Maxwell fluid with a purely viscous element (eq. (40)). The equivalence between eqs. (40) and (72) comes from the fact that the contribution from the Basset force to the frequency-dependent friction, the second term of the right side of eq. (65), gives the constant $6\pi R^2\sqrt{\rho g} = H/\omega_M (:= \zeta_M)$ at $\omega \gg 1/\lambda$ that plays the same role as a constant, pure viscosity. Thus the inclusion of the Basset force alone corresponds to the inclusion of an effective pure viscosity ζ_M, thereby eliminating the peak in the PSD and the oscillation in the MSD. As shown below, even when the effective bead mass is considered, the peak in the PSD does not appear if the bead density and the fluid density are comparable. Equation (72) is roughly expressed as

$$I(\omega) \simeq \frac{6k_{\rm B}T}{\zeta} \times \begin{cases} \omega^{-2} & (\omega \ll \sqrt{\omega_M/\lambda}) \\ \lambda/\omega_M & (\sqrt{\omega_M/\lambda} \ll \omega \ll \omega_M) \\ \lambda\omega_M\omega^{-2} & (\omega_M \ll \omega) \end{cases}. \tag{73}$$

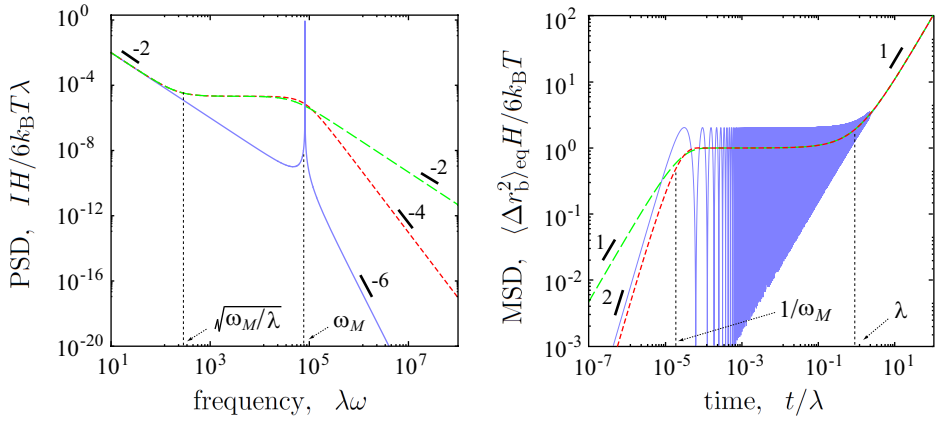

FIG. 8. (color online). The power spectral density (left) and the mean-square displacement (right) of a bead in the Maxwell fluid with effects of the Basset force alone (dashed green line), and effective bead mass alone (solid blue line), and the Basset force and effective bead mass (dotted red line). $M = m = 10^{-10}\lambda\zeta$.

See Fig. 8 (dashed line of the left figure). There appears a plateau at $\sqrt{\omega_M/\lambda} \ll \omega \ll \omega_M$, and the bead moves diffusively both in lower ($\omega \ll \sqrt{\omega_M/\lambda}$) and higher ($\omega \gg \omega_M$) frequency regimes. The corresponding MSD is

$$\left\langle \Delta r_{\rm b}^2[\omega] \right\rangle_{\rm eq} \simeq \frac{6k_{\rm B}T}{H}\left(1 + \frac{t}{\lambda} - e^{-\omega_M t}\right) \tag{74}$$

$$\simeq \frac{6k_{\rm B}T}{H} \times \begin{cases} \omega_M t & (t \ll 1/\omega_M) \\ 1 & (1/\omega_M \ll t \ll \lambda) \\ t/\lambda & (t \gg \lambda) \end{cases} \tag{75}$$

where $\omega_M \gg 1/\lambda$ was assumed in deriving these equations. See also Fig. 8 (dashed line of the right figure). Since the MSD does not oscillate, effects of the Basset force can be erased in a naïve way simply by taking a limit $M \to 0$ (*i.e.*, $\omega_M \to \infty$).

2. *Effective bead mass*

In the absence of the Basset force, inertial effects of the bead and the fluid dragged around with it is qualitatively the same as that of the bare bead. The only difference is that bead mass m is replaced with $m_{\rm eff}$ in which mass of the dragged fluid is included. Therefore, as discussed in Sec. II C, the inertial time scale is given by the inverse of the frequency $\omega_{m_{\rm eff}} := \sqrt{H/m_{\rm eff}}$. If

$m \simeq M$ then $\omega_{m_{\rm eff}} \simeq \omega_M$, and the PSD is roughly expressed as (see Fig. 8)

$$I(\omega) \simeq \frac{6k_{\rm B}T}{\zeta} \times \begin{cases} \omega^{-2} & (\omega \ll \omega_M) \\ \lambda^2 & (\omega \simeq \omega_M) \\ \omega_M^4 \omega^{-6} & (\omega_M \ll \omega) \end{cases} . \tag{76}$$

The peak appearing at $\omega \simeq \omega_M$ cannot be neglected safely by the limit $m \simeq M \to 0$; it just moves towards higher frequencies while keeping its height and width constant, and never disappears.

3. Combined effects of fluid inertia

Finally, we examine the influence of the Basset force together with the inertia of the dragged fluid on the PSD. Substituting eq. (68) into eq. (71), we obtain

$$I(\omega) \simeq \frac{6k_{\rm B}T}{\zeta} \frac{\lambda\omega_M}{\omega^2} \frac{\omega^2 + \omega/\lambda_M}{(\lambda m_{\rm eff}\omega_M/\zeta)^2\omega^4 + \left[(m_{\rm eff}\omega_M/\zeta + 1)^2 - 2\lambda m_{\rm eff}\omega_M^2/\zeta\right]\omega^2 + \omega_M^2} \qquad (\omega \gg 1/\lambda). \tag{77}$$

As before, we can assume conditions $\omega_M \gg 1/\lambda$ and $m_{\rm eff} \ll \lambda\zeta$. If $m \simeq M$, then $\omega_m \simeq \omega_M$ and eq. (77) is approximately written as

$$I(\omega) \simeq \frac{6k_{\rm B}T}{\zeta} \frac{\lambda\omega_M^3(\omega^2 + \omega_M/\lambda)}{\omega^2(\omega^4 + \omega_M^2\omega^2 + \omega_M^4)} \tag{78}$$

$$\simeq \frac{6k_{\rm B}T}{\zeta} \times \begin{cases} \omega^{-2} & (\omega \ll \sqrt{\omega_M/\lambda}) \\ \lambda/\omega_M & (\sqrt{\omega_M/\lambda} \ll \omega \ll \omega_M) \\ \lambda\omega_M^3\omega^{-4} & (\omega_M \ll \omega) \end{cases} . \tag{79}$$

The only difference with eq. (73) is that the power of the PSD is -4 (ballistic) rather than -2 (diffusive) in the high frequency regime $\omega \gg \omega_M$. See Fig. 8 where numerically calculated MSDs corresponding to eq. (77) are also shown. Some cases where M is not equal to m are depicted in Fig. 9 as a reference. With increasing M toward m, a peak in the PSD decreases (or the oscillation of the MSD attenuates) and it disappears if both masses are comparable. Thus the inertial effects of both fluid and bead can be erased in a naïve way simply by taking a limit $M \to 0$ with keeping $M \simeq m$. If $M \simeq m$ and therefore there is no peak in the PSD (or no oscillation in the MSD), an inclusion of the purely viscous element with infinitesimal viscosity causes only an infinitesimal change in the PSD (and the MSD).

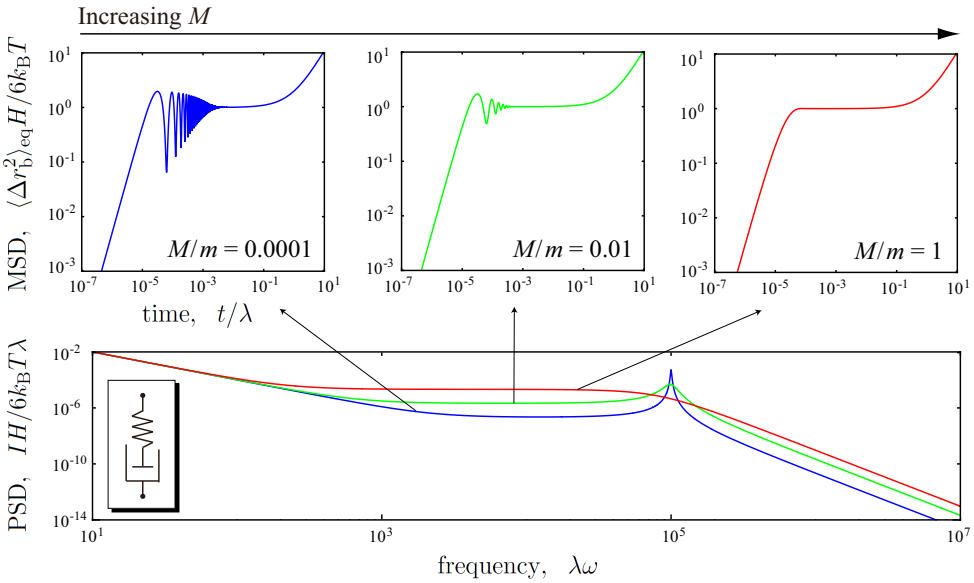

FIG. 9. (color online). The mean-square displacement and the corresponding power spectral density of a bead in the Maxwell fluid. Fluid mass per bead volume M is different for each curve with a fixed bead mass $m = 10^{-10}\lambda\zeta$.

IV. CONCLUSION

We studied the effects of inertia of both tracer bead and medium on the positional autocorrelation of the bead (mean-square displacement and power spectral density) for a single-mode Maxwell fluid and its extension. By introducing a small amount of bead mass in the generalized Stokes-Einstein relation, the mean-square displacement of the bead oscillates drastically at time regimes smaller than, but comparable to, the relaxation time of the fluid. The frequency of oscillation diverges in the zero limit of bead mass. However, if we include a purely viscous element with infinitesimal viscosity in the dynamic modulus, inertia can be eliminated safely thereby recovering the result from the GSER without bead inertia, but with proper initial condition. An anomalous gap indicated by McKinley *et al.* between the inertia-less MSD (this is different from the one from Mason-Weitz's GSER) and the MSD for finite bead mass also disappears in the presence of the purely viscous element. The anomalous gap of the MSD corresponds to the area of the inertial peak in the PSD that is eliminated in the naïve zero-mass limit.

In real Maxwell fluids such as wormlike micelle solutions, there exists a relaxation spectrum outside the window where a single-mode Maxwell behavior is observed. Such a spectrum attenuates the oscillation of bead displacement at the corresponding time regime inside the window. We studied the two-mode Maxwell model to find the condition necessary for such a suppression of

the oscillation. It was shown that if bead mass is smaller than a specific mass determined by the viscoelastic parameters, oscillation is pushed outside the window and decays inside the window. The oscillation never disappears outside the window. But if there were a third Maxwell mode whose relaxation time is smaller than that of the second mode, the oscillation would shift further towards the shorter time regime. In general, we expect that the broader the relaxation spectrum, the smaller the time regime where the oscillation takes place in the MSD.

Fluid inertia affects the bead autocorrelation through both the fluid dragged around with the bead and the Basset force. The former generates a peak in PSD (or oscillation of MSD) while the latter does not. Actually, the Basset force plays the same role as the purely viscous element at high frequencies where the storage modulus exhibits the plateau. If fluid density and bead density are comparable, the Basset force suppresses the peak in the PSD.

All these factors, *i.e.*, the existence of a purely viscous component, relaxation modes at high frequencies, and medium inertia tend to bury the oscillations of the MSD inside an experimental window in the noise level of particle-tracking measurements.

We are grateful to the National Science Foundation (grant NSF-SCI 05063059) and the Army Research Office (grants W911NF-08-2-0058 and W911NF-09-1-0378) for financial support.

Appendix A: The two-mode Maxwell fluids

Here we detail MSD behavior of the bead in the two-mode Maxwell fluids discussed in Sec. II E for each side of the e-1M window.

1. Inside the e-1M window ($t \gg \lambda_2$)

By taking the inverse one-sided Fourier transform of eq. (50), MSD inside the e-1M time window is obtained as

$$\begin{aligned}\left\langle \Delta r_{\mathrm{b}}^2(t) \right\rangle_{\mathrm{eq}}^{(1)} =& \frac{6k_{\mathrm{B}}T}{H_1}\left(\frac{\zeta_1}{\zeta_1+\zeta_2}\right)^2 \\ &\times \begin{cases} 1 + t/\tau_{\mathrm{d}}^{(1)} - \left(\frac{1+B_m^{(1)}}{2} e^{-t/\tau_{\mathrm{e}}^{(1)}} + \frac{1-B_m^{(1)}}{2} e^{-t/\tau_{\mathrm{b}}^{(1)}}\right) & (\text{for } \; m < m_c^{(1)}) \\ 1 + t/\tau_{\mathrm{d}}^{(1)} - e^{-t(1/\tau_{\mathrm{e}}^{(1)}+1/\tau_{\mathrm{b}}^{(1)})/2}\left(\cos\omega_m^{(1)} t + B_m^{(1)\prime} \sin\omega_m^{(1)} t\right) & (\text{for } \; m > m_c^{(1)}) \end{cases}\end{aligned} \tag{A1}$$

where

$$\tau_{\mathrm{d}}^{(1)} := \frac{\zeta_1\lambda_1}{\zeta_1+\zeta_2} \tag{A2}$$

is the time constant associated with the diffusive motion of the tracer bead, and the coefficients are given by

$$B_m^{(1)} := \frac{C^{(1)}}{\lambda_1\zeta_1\sqrt{(\lambda_1\zeta_2+\lambda_2\zeta_1+m)^2-4m\lambda_1(\zeta_1+\zeta_2)}}, \tag{A3a}$$

$$B_m^{(1)\prime} := -iB_m^{(1)} = \frac{C^{(1)}}{2m\lambda_1^2\zeta_1\omega_m^{(1)}} \tag{A3b}$$

with $C^{(1)} := (\lambda_1\zeta_2+\lambda_2\zeta_1+m)^2-\lambda_1(\zeta_1+\zeta_2)(\lambda_1\zeta_2+\lambda_2\zeta_1+3m)$.

In eq. (A1),

$$m_c^{(1)} := \lambda_1\zeta_1\left(\sqrt{1+\zeta_2/\zeta_1}-1\right)^2 \tag{A4}$$

is the critical mass defined from the zero-point of the square-root in the denominator of eq. (51). If bead mass is so small as to satisfy the condition $m < m_c^{(1)}$, then the argument of the square-root is positive, so that $\tau_{\rm b,e}^{(1)}$ have a real value indicating that the MSD does not oscillate inside the e-1M window. The condition $\tau_{\rm b}^{(1)} < \tau_{\rm e}^{(1)} < \tau_{\rm d}^{(1)}$ is always satisfied, but the relaxation time of the ballistic mode $\tau_{\rm b}^{(1)}$ can be placed inside ($\lambda_2 < \tau_{\rm b}^{(1)}$) or outside ($\tau_{\rm b}^{(1)} < \lambda_2$) the e-1M window depending on the value of bead mass. In the former case ($\lambda_2 < \tau_{\rm b}^{(1)}$), the ballistic mode appears inside the e-1M window followed by the diffusive mode up to $\tau_{\rm e}^{(1)}$ due to the viscous component of the second Maxwell element (see figure b of Fig. 6), while in the latter case ($\tau_{\rm b}^{(1)} < \lambda_2$), it does not and only the diffusive mode appears (see figures c-1 and c-2 of Fig. 6). For both cases, a plateau appears with its height $\langle r_{\rm b}(t)^2\rangle_{\rm eq} = \frac{6k_{\rm B}T}{H_1}\left(\frac{\zeta_1}{\zeta_1+\zeta_2}\right)^2$ for $\tau_{\rm e}^{(1)} \ll t \ll \tau_{\rm d}^{(1)}$, and the bead diffuses as $\langle r_{\rm b}(t)^2\rangle_{\rm eq} = \frac{6k_{\rm B}T}{\zeta_1+\zeta_2}t$ at the longest time regime $t \gg \tau_{\rm d}^{(1)}$. (The precise expression of the plateau is $6k_{\rm B}T\frac{\lambda_1\zeta_1+\lambda_2\zeta_2}{(\zeta_1+\zeta_2)^2}$. Since the second term of the denominator can be neglected in the current condition $\lambda_1 \gg \lambda_2$, this is approximately expressed as $6k_{\rm B}T\frac{\lambda_1\zeta_1}{(\zeta_1+\zeta_2)^2} \simeq \frac{6k_{\rm B}T}{H_1}(\frac{\zeta_1}{\zeta_1+\zeta_2})^2$.) An important point here is that if ζ_2 is much smaller than ζ_1, the GSER's result is recovered at $t \gg \tau_{\rm e}^{(1)}$ that exists inside the e-1M window.

With increasing m, the onset $\tau_b^{(1)}$ and the terminal $\tau_e^{(1)}$ of the internal diffusive mode approach, and if $m = m_c^{(1)}$, both become equal with each other thereby eliminating this diffusive mode. When $m > m_c^{(1)}$, these times take a complex value, and therefore the MSD oscillates. The imaginary part of their inverse gives the frequency of the oscillation:

$$\omega_m^{(1)} := \frac{\sqrt{4m\lambda_1(\zeta_1+\zeta_2)-(\lambda_1\zeta_2+\lambda_2\zeta_1+m)^2}}{2m\lambda_1}. \tag{A5}$$

Instead of $\tau_{b,e}^{(1)}$ themselves, their mean times

$$\sqrt{\tau_{\rm b}^{(1)}\tau_{\rm e}^{(1)}} = \sqrt{\frac{m\lambda_1}{\zeta_1+\zeta_2}} =: \lambda_{\rm b}^{(1)}, \tag{A6}$$

$$\frac{2}{1/\tau_{\rm b}^{(1)}+1/\tau_{\rm e}^{(1)}} = \frac{m\lambda_1}{\lambda_1\zeta_2+\lambda_2\zeta_1+m} =: \lambda_{\rm e}^{(1)} \tag{A7}$$

describe the dynamics of bead displacement in this case. These times always satisfy the conditions $\lambda_2 < \lambda_{\rm b}^{(1)} < \lambda_{\rm e}^{(1)} < \tau_{\rm d}^{(1)}$ [38]. In the smaller time regime $t \ll \lambda_{\rm b}^{(1)}$, the bead displacement is ballistic. (This mode is also dominant at all time regime outside the e-1M window.) The oscillation is observed for $\lambda_{\rm b}^{(1)} \ll t \lesssim \lambda_{\rm e}^{(1)}$ while gradually decreasing its amplitude as times goes on because of the energy dissipation by the viscous elements. After the oscillation is attenuated, a plateau appears for $\lambda_{\rm e}^{(1)} \ll t \ll \tau_{\rm d}^{(1)}$. The bead diffuses away at the longest time regime $t \gg \tau_{\rm d}^{(1)}$. These behavior can be confirmed in figures a-1 and a-2 in Fig. 6.

2. Outside the e-1M window ($t \ll \lambda_2$)

The MSD of the bead outside the e-1M window is obtained from eq. (52) as follows

$$\begin{aligned}\left\langle \Delta r_{\rm b}^2(t)\right\rangle_{\rm eq}^{(2)} =& \frac{6k_{\rm B}T}{H_1}\frac{\lambda_2\zeta_1}{\lambda_1\zeta_2+\lambda_2\zeta_1+m} \\ &\times \begin{cases} 1-\left(\frac{1+B_m^{(2)}}{2}e^{-t/\tau_{\rm e}^{(2)}} + \frac{1-B_m^{(2)}}{2}e^{-t/\tau_{\rm b}^{(2)}}\right) & (\text{for } \ m > m_c^{(2)}) \\ 1-e^{-t/(2\lambda_2)}(\cos\omega_m^{(2)}t + B_m^{(2)\prime}\sin\omega_m^{(2)}t) & (\text{for } \ m < m_c^{(2)}) \end{cases}\end{aligned} \tag{A8}$$

where the coefficients are given by

$$B_m^{(2)} := \sqrt{\frac{m\lambda_1}{m\lambda_1 - 4\lambda_2(\lambda_1\zeta_2+\lambda_2\zeta_1+m)}}, \tag{A9a}$$

$$B_m^{(2)\prime} := -iB_m^{(2)} = \frac{1}{2\lambda_2\omega_m^{(2)}} \tag{A9b}$$

with

$$\omega_m^{(2)} := \frac{\sqrt{4m\lambda_1\lambda_2(\lambda_1\zeta_2+\lambda_2\zeta_1+m)-(m\lambda_1)^2}}{2m\lambda_1\lambda_2}, \tag{A10}$$

and the critical mass is

$$m_c^{(2)} := 4\frac{\lambda_2}{\lambda_1}(\lambda_1\zeta_2+\lambda_2\zeta_1). \tag{A11}$$

If $m > m_c^{(2)}$, the argument of the square-root of $\tau_{\rm b,e}^{(2)}$ given by eq. (53) is positive, so that $\tau_{\rm b,e}^{(2)}$ take a real value and the MSD does not oscillate. A condition $\lambda_2 < \tau_{\rm b}^{(2)} < \tau_{\rm e}^{(2)}$ holds. The first inequality

assures that the bead displacement is ballistic at all time regimes outside the e-1M window (figures a-1, a-2 and b in Fig. 6).

On the other hand, if bead mass is so small that the condition $m < m_c^{(2)}$ is fulfilled, $\tau_{\rm b,e}^{(2)}$ take a complex value and the MSD oscillates with the frequency $\omega_m^{(2)}$. With decreasing bead mass, the frequency becomes high as $\omega_m^{(2)} \simeq \sqrt{\frac{\lambda_1\zeta_2+\lambda_2\zeta_1}{m\lambda_1\lambda_2}}$, and it diverges in the zero-mass limit. Therefore, the oscillation never disappears *outside* the e-1M window, although its effects disappear inside the e-1M window as explained above. The bead's displacement is governed by the following characteristic times given as the means of $\tau_{b,e}^{(2)}$:

$$\sqrt{\tau_{\rm b}^{(2)}\tau_{\rm e}^{(2)}} = \sqrt{\frac{m\lambda_1\lambda_2}{\lambda_1\zeta_2+\lambda_2\zeta_1+m}} =: \lambda_{\rm b}^{(2)}, \tag{A12}$$

$$\frac{2}{1/\tau_{\rm b}^{(2)}+1/\tau_{\rm e}^{(2)}} = 2\lambda_2 =: \lambda_{\rm e}^{(2)}. \tag{A13}$$

These times always satisfy the condition $\lambda_{\rm b}^{(2)} < \lambda_2 < \lambda_{\rm e}^{(2)}$ [39]. The displacement of the bead is ballistic at the shortest time regime $t \ll \lambda_{\rm b}^{(2)}$, and oscillates in the rest of the regime: $\lambda_{\rm b}^{(2)} \ll t \lesssim \lambda_{\rm e}^{(2)}$ ($\sim \lambda_2$). See also figures c-1 and c-2 in Fig. 6.

[1] T. G. Mason and D. A. Weitz, Physical Review Letters **74**, 1250 (1995).

[2] A. Mukhopadhyay and S. Granick, Current Opinion in Colloid & Interface Science **6**, 423 (2001).

[3] T. A. Waigh, Reports on Progress in Physics **68**, 685 (2005).

[4] S. Yamada, D. Wirtz, and S. C. Kuo, Biophysical Journal **78**, 1736 (2000).

[5] E. M. Furst, Current Opinion in Colloid & Interface Science **10**, 79 (2005).

[6] Y. Kimura, Journal of the Physical Society of Japan **78**, 041005 (2009).

[7] T. M. Squires and T. G. Mason, Annual Review of Fluid Mechanics **42**, 413 (2010).

[8] R. B. Bird, R. C. Armstrong, and O. Hassager, *Dynamics of Polymeric Liquids Vol II: Kinetic Theory*, 2nd ed. (Addison-Wesley, New York, 1987).

[9] T. G. Mason, Rheologica Acta **39**, 371 (2000).

[10] J. H. van Zanten and K. P. Rufener, Physical Review E **62**, 5389 (2000).

[11] T. Savin and P. S. Doyle, Physical Review E **71**, 041106 (2005).

[12] S. A. McKinley, L. Yao, and M. G. Forest, Journal of Rheology **53**, 1487 (2009).

[13] J. Fricks, L. Yao, T. C. Elston, and M. G. Forest, SIAM Journal on Applied Mathematics **69**, 1277 (2009).

[14] M. Buchanan, M. Atakhorrami, J. F. Palierne, F. C. MacKintosh, and C. F. Schmidt, Physical Review E **72**, 011504 (2005).

[15] N. Willenbacher, C. Oelschlaeger, M. Schopferer, P. Fischer, F. Cardinaux, and F. Scheffold, Physical Review Letters **99**, 068302 (2007).

[16] J. Galvan-Miyoshi, J. Delgado, and R. Castillo, European Physical Journal E **26**, 369 (2008).

[17] A. Amitai, Y. Kantor, and M. Kardar, Physical Review E **81**, 011107 (2010).

[18] C. Oelschlaeger, P. Suwita, and N. Willenbacher, Langmuir **26**, 7045 (2010).

[19] N. van Kampen, Brazilian Journal of Physics **28**, 90 (1998).

[20] R. Kubo, M. Toda, and N. Hashitsume, *Statistical Physics II: Nonequilibrium Statistical Mechanics* (Springer-Verlag, Berlin, 1985).

[21] L. D. Landau and E. M. Lifshitz, *Statistical Physics, Part 1*, 3rd ed., Vol. 5 (Butterworth-Heinmann, UK, 1980).

[22] H. Rehage and H. Hoffmann, Journal of Physical Chemistry **92**, 4712 (1988).

[23] T. Annable, R. Buscall, R. Ettelaie, and D. Whittlestone, Journal of Rheology **37**, 695 (1993).

[24] J. P. Hansen and I. R. McDonald, *Theory of Simple Liquids*, 3rd ed. (Academic Press, London, 2006).

[25] T. Li, S. Kheifets, D. Medellin, and M. G. Raizen, Science **328**, 1673 (2010).

[26] G. E. Uhlenbeck and L. S. Ornstein, Physical Review **36**, 823 (1930).

[27] J. Z. Xue, D. J. Pine, S. T. Milner, X. l. Wu, and P. M. Chaikin, Physical Review A **46**, 6550 (1992).

[28] A. J. Levine and T. C. Lubensky, Physical Review Letters **85**, 1774 (2000).

[29] B. Schnurr, F. Gittes, F. C. MacKintosh, and C. F. Schmidt, Macromolecules **30**, 7781 (1997).

[30] K. Xu, M. G. Forest, and I. Klapper, Journal of Non-Newtonian Fluid Mechanics **145**, 150 (2007).

[31] R. Zwanzig and M. Bixon, Physical Review A **2**, 2005 (1970).

[32] E. H. Lee, Quarterly of Applied Mathematics **13**, 183 (1955).

[33] L. D. Landau and E. M. Lifshitz, *Fluid Mechanics*, 2nd ed., Vol. 6 (Butterworth-Heinemann, UK, 1987).

[34] E. E. Michaelides, Journal of Fluids Engineering **125**, 209 (2003).

[35] H. Lamb, *Hydrodynamics*, sixth ed. (Dover Publications, USA, 1932).

[36] T. B. Liverpool and F. C. MacKintosh, Physical Review Letters **95**, 208303 (2005).

[37] N. Willenbacher and C. Oelschlaeger, Current Opinion in Colloid & Interface Science **12**, 43 (2007).

[38] $\tau_{\rm d}^{(1)} - \lambda_{\rm e}^{(1)} = \lambda_1\zeta_1(\lambda_1\zeta_2 + \lambda_2\zeta_1)/[(\zeta_1+\zeta_2)(\lambda_1\zeta_2 + \lambda_2\zeta_1 + m)]) > 0$, $(\lambda_{\rm b}^{(1)})^2 - (\lambda_2)^2 = [m\lambda_1 - (\zeta_1 + \zeta_2)(\lambda_2)^2]/(\zeta_1+\zeta_2) > (\lambda_1)^2\zeta_1(\sqrt{1+\zeta_2/\zeta_1} - 1)^2/(\zeta_1+\zeta_2) > 0$ where an inequality $m > m_c^{(1)}$ was used.

[39] $(\lambda_2)^2 - (\lambda_{\rm b}^{(2)})^2 = (\lambda_2)^2(\lambda_1\zeta_2 + \lambda_2\zeta_1 - m)/(\lambda_1\zeta_2 + \lambda_2\zeta_1 + m) > 0$ where bead mass was assumed to be small.